

AD-A106 744

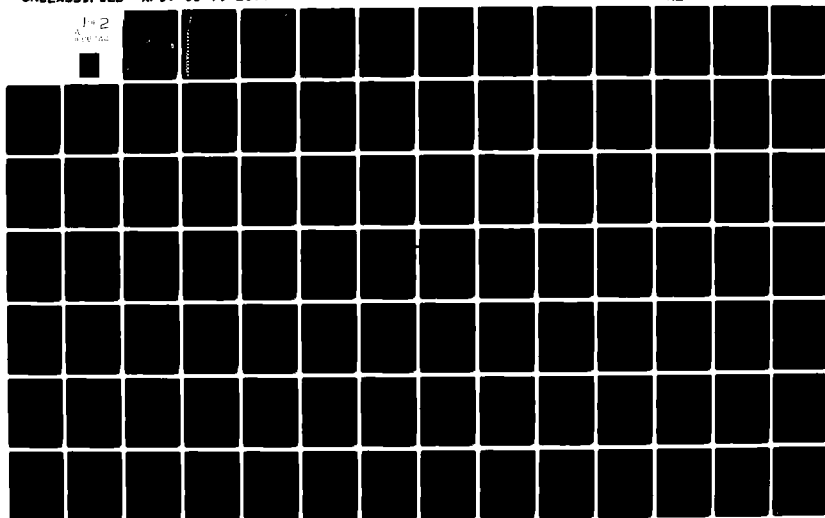
AIR FORCE INST OF TECH WRIGHT-PATTERSON AFB OH
THE OCCURRENCE AND GEOLOGICAL IMPLICATIONS OF CARBON DIOXIDE CL--ETC(U)
MAY 79 6 A ARMISTEAD
AFIT-CI-79-257T

F/6 3/2

UNCLASSIFIED

NL

1-2
3-10-79



UNCLASS

SECURITY CLASSIFICATION OF THIS PAGE (When Data Entered)

REPORT DOCUMENTATION PAGE		READ INSTRUCTIONS BEFORE COMPLETING FORM
1. REPORT NUMBER 79-257T	2. GOVT ACCESSION NO. AD-A106744	3. RECIPIENT'S CATALOG NUMBER 744
4. TITLE (and Subtitle) The Occurrence and Geological Implications of Carbon Dioxide Clathrate Hydrate on Mars.		5. TYPE OF REPORT & PERIOD COVERED THESIS/DISSERTATION
6. AUTHOR(S) Gary Anthony/Armistead		6. PERFORMING ORG. REPORT NUMBER
7. PERFORMING ORGANIZATION NAME AND ADDRESS AFIT STUDENT AT: University of Houston		8. CONTRACT OR GRANT NUMBER(s)
9. CONTROLLING OFFICE NAME AND ADDRESS AFIT/NR WPAFB OH 45433		10. PROGRAM ELEMENT, PROJECT, TASK AREA & WORK UNIT NUMBERS 11
14. MONITORING AGENCY NAME & ADDRESS (if different from Controlling Office) LEVEL II		12. REPORT DATE May 1979
		13. NUMBER OF PAGES 96
		15. SECURITY CLASS. (of this report) UNCLASS
16. DISTRIBUTION STATEMENT (of this Report) APPROVED FOR PUBLIC RELEASE; DISTRIBUTION UNLIMITED (14) AF 7-01-79-257T		15a. DECLASSIFICATION/DOWNGRADING SCHEDULE DTIC ELECTE NOV 6 1981 D
17. DISTRIBUTION STATEMENT (of the abstract entered in Block 20, if different from Report) 20 OCT 1981		H 20 OCT 1981
18. SUPPLEMENTARY NOTES APPROVED FOR PUBLIC RELEASE: IAW AFR 190-17		FREDRIC C. LYNCH, Major, USAF Director of Public Affairs Air Force Institute of Technology (AFIT) Wright-Patterson AFB, OH 45433
19. KEY WORDS (Continue on reverse side if necessary and identify by block number)		
20. ABSTRACT (Continue on reverse side if necessary and identify by block number) ATTACHED		

81 10 26 145

012201

AD A106744

DTIC FILE COPY

ABSTRACT

Carbon dioxide

Analysis of the temperatures and pressures at the Viking Lander 2 site (VL-2) during the presence of surface ice condensate shows that the ice partially converted to CO_2 clathrate hydrate on at least several occasions. The occurrence of CO_2 hydrate at the VL-2 latitude indicates that ground ice and surface ice at latitudes nearer the poles would convert to hydrate during the Martian winter. The conversion of ice to hydrate is shown to result in a volume expansion of $16\% + 2\%$ ~~2%~~. The geological importance of this volume expansion, and the converse volume reduction as hydrate converts to ice, is investigated. The reduction in volume appears to be a good candidate for the cause of the chaotic terrain. A method is suggested for determining whether the melting of a buried deposit of ice or the dissociation of a buried hydrate deposit, and subsequent melting of the resulting ice, caused the chaotic terrain and associated flood channels. No quantitative measure of the force exerted by ice as it converts to hydrate was obtained. However, calculations indicate that the conversion of ice to hydrate could approach the force given by the freezing of water in confined spaces provided sufficient time is allowed for the reaction and the ice completely fills the confined space prior to conversion. The measurement of strains imparted to walls confining a solid ice mass as it converts to hydrate is necessary before the process can be advanced as a possible geomorphological and weathering agent on Mars.

Accession For	RTIS CP:AI	DTIC TAB	Unannounced	Justification
			<input type="checkbox"/>	<input type="checkbox"/>
BY	Distribution/	Availability Codes	Dist	Special

~~79-132T~~
79-257T

THE OCCURRENCE AND GEOLOGICAL IMPLICATIONS
OF CARBON DIOXIDE CLATHRATE HYDRATE
ON MARS

A Thesis Presented to the Faculty
of the Department of Geology,
University of Houston

In Partial Fulfillment
of the Requirements for the Degree
Master of Science

by

Gary Anthony Armistead

May, 1979

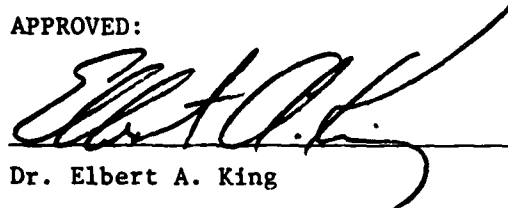
81 10 26 145

THE OCCURRENCE AND GEOLOGICAL IMPLICATIONS
OF CARBON DIOXIDE CLATHRATE HYDRATE
ON MARS

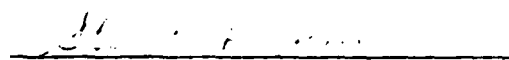
by

Gary Anthony Armistead

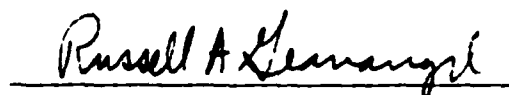
APPROVED:



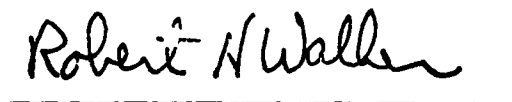
Dr. Elbert A. King



Dr. Stuart A. Hall



Dr. Russell A. Geanangel



Dr. Robert H. Walker
Dean, College of Natural Sciences
and Mathematics

THE OCCURRENCE AND GEOLOGICAL IMPLICATIONS
OF CARBON DIOXIDE CLATHRATE HYDRATE
ON MARS

An Abstract of a Thesis
Presented to
the Faculty of the Department of Geology
the University of Houston
in Partial Fulfillment
of the Requirements for the
Degree of Master of Science

by

Gary Anthony Armistead

May, 1979

TABLE OF CONTENTS

	Page
ABSTRACT	11
INTRODUCTION AND PREVIOUS WORK	1
CO ₂ CLATHRATE HYDRATE ON MARS: A PRE-VIKING ASSESSMENT	7
A VIKING ASSESSMENT OF CO ₂ HYDRATE OCCURRENCE ON MARS.	25
GEOLOGICAL IMPLICATIONS OF CO ₂ HYDRATE OCCURRENCE ON MARS.	44
Volume Changes of CO ₂ Hydrate Formation and Dissociation.	44
CO ₂ Hydrate Dissociation and Martian Geomorphology.	59
CO ₂ Hydrate Formation and Martian Geomorphology	61
Summary	84
APPENDIX 1	86
APPENDIX 2	90
APPENDIX 3	92
ACKNOWLEDGEMENTS	95
REFERENCES	96

ABSTRACT

Analysis of the temperatures and pressures at the Viking Lander 2 site (VL-2) during the presence of surface ice condensate shows that the ice partially converted to CO_2 clathrate hydrate on at least several occasions. The occurrence of CO_2 hydrate at the VL-2 latitude indicates that ground ice and surface ice at latitudes nearer the poles would convert to hydrate during the Martian winter. The conversion of ice to hydrate is shown to result in a volume expansion of $16\% \pm 2\%$. The geological importance of this volume expansion, and the converse volume reduction as hydrate converts to ice, is investigated. The reduction in volume appears to be a good candidate for the cause of the chaotic terrain. A method is suggested for determining whether the melting of a buried deposit of ice or the dissociation of a buried hydrate deposit, and subsequent melting of the resulting ice, caused the chaotic terrain and associated flood channels. No quantitative measure of the force exerted by ice as it converts to hydrate was obtained. However, calculations indicate that the conversion of ice to hydrate could approach the force given by the freezing of water in confined spaces provided sufficient time is allowed for the reaction and the ice completely fills the confined space prior to conversion. The measurement of strains imparted to walls confining a solid ice mass as it converts to hydrate is necessary before the process can be advanced as a possible geomorphological and weathering agent on Mars.

INTRODUCTION AND PREVIOUS WORK

Clathrates are compounds in which nonbonded "guest" molecules are physically trapped in cages formed by the host lattice (Sill and Wilkening, 1978). The molecules forming the crystal lattice do not specifically interact with the "guest" molecules (Miller, 1974). The interaction is limited to the van der Waals type even for polar "guest" molecules (Davidson, 1973). The clathrate hydrates, also called gas hydrates, are a special case of clathrate compounds in which an expanded water ice lattice forms cages that contain gas molecules (Miller, 1974). Reviews of clathrate hydrates have been given by van der Waals and Platteeuw (1959), Jeffrey and McMullan (1967), Davidson (1973), and Miller (1974).

The first clathrate hydrate was discovered by Sir Humphry Davy (Davy, 1811). He observed crystals of an ice-like material formed when an aqueous solution saturated with chlorine gas was cooled to below 9°C. During the period 1880-1910, Villard and de Forcrand, and others, investigated a number of gases that formed hydrates. Schroeder (1926) has published a detailed review of the work with clathrate hydrates before 1926. The field of investigation remained largely dormant until 1935-1945 when the clathrates of natural gas were found to precipitate in and clog up natural gas pipelines (Hammerschmidt, 1934; Deaton and Frost, 1946).

Modern investigations of clathrate hydrates began with the work of von Stackelberg and co-workers (1949-1954).

These investigations included thermodynamic, composition, and X-ray studies. Von Stackelberg (1949) showed by X-ray diffraction that there were two types of gas hydrates (Structure I and Structure II). The first determination of the Structure I hydrate was done by Pauling and Marsh (1952). The correct structure for the Structure II hydrates was guessed by model building (Claussen 1951a, b) and later confirmed by X-ray diffraction (von Stackelberg and Muller, 1951; Mak and McMullan, 1965).

The determinant of which hydrate structure will form is the size of the gas molecule to be encaged (Miller, 1974; Davidson, 1973). Figure 1 shows the relationship of the particular hydrate type to the size of the "guest" molecule.

The framework of the Structure I hydrate is shown in Figure 2. There are 46 water molecules in a 12 Å cubic unit cell that form 2 pentagonal dodecahedra (12 sided polyhedron) and 6 tetrakaidecahedra (14 sided polyhedron) (Davidson, 1973). Molecules 5.1 Å or less in diameter will fit into the pentagonal dodecahedra and molecules 5.8 Å or less in diameter will fit into the tetrakaidecahedra (Miller, 1974). The ideal formula for a hydrate with both types of cages filled is $X \cdot 5.75 \text{ H}_2\text{O}$ (where X represents one gas molecule) (Davidson, 1973). Actual formulas, however, differ from the ideal formulas because the cages are not 100% occupied by gas molecules. This determination is based on the statistical mechanical treatment of the gas hydrates by van der Waals and Platteeuw (1959), Barrer and Stuart (1957), and McKoy and Sinanoglu (1963). However, for most hydrates the actual

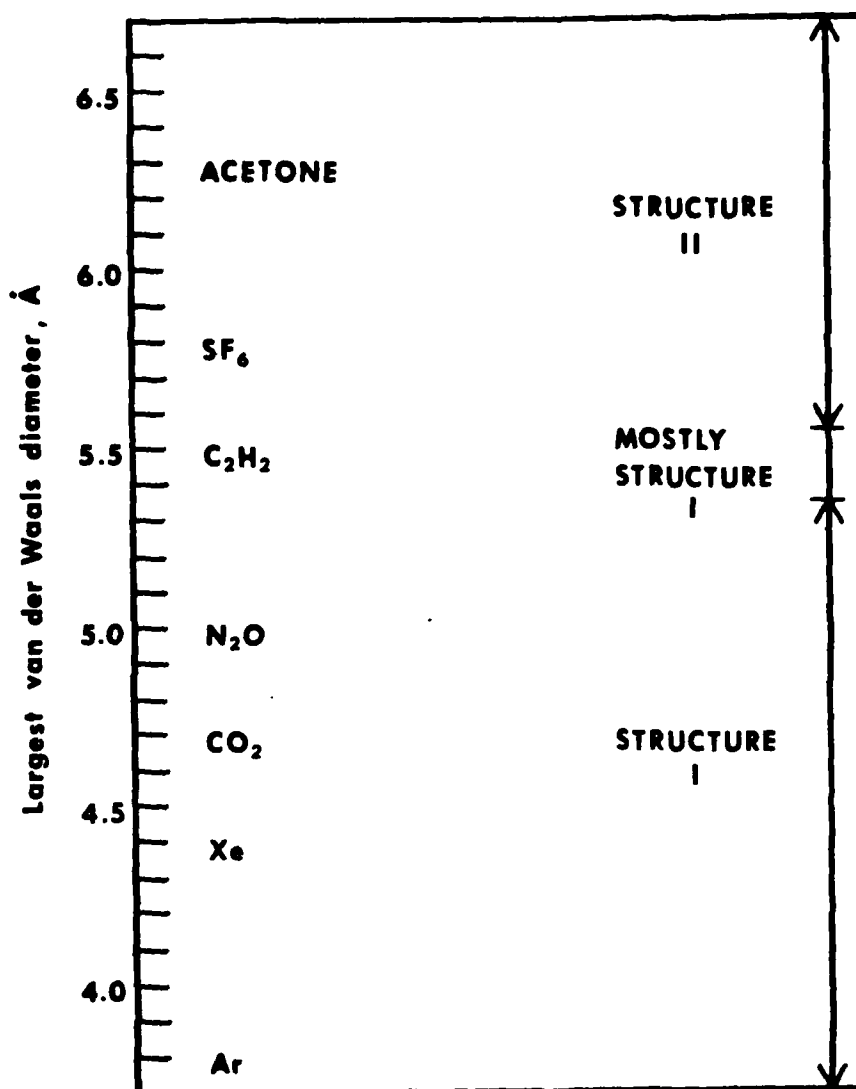


Fig. 1. Some molecules which form clathrate hydrates, arranged in order of size. (After Davidson, 1973).

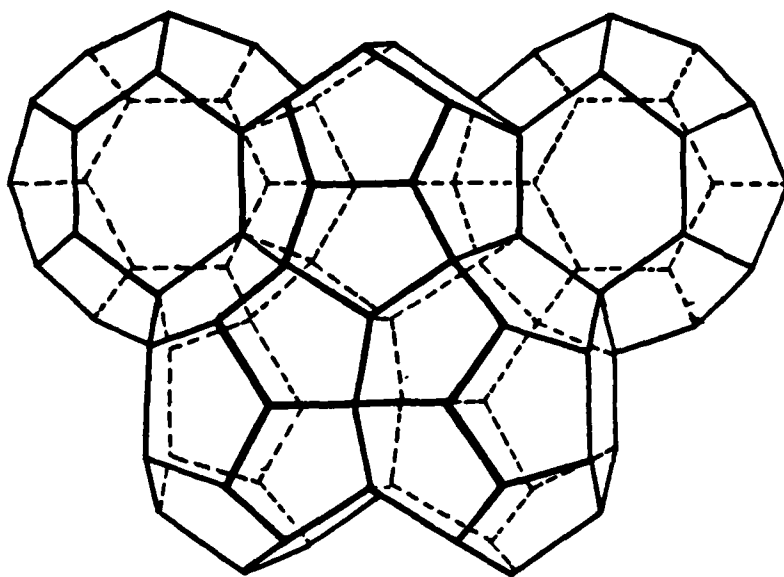


Fig. 2. The 12 Å Structure I Hydrate. The pentagonal dodecahedron (upper center) is formed by 20 water molecules. The tetrakaidecahedra is formed by 24 water molecules and have 2 opposite hexagonal faces and 12 pentagonal faces (After Miller, 1974).

formula is not far from the ideal formula (Miller, 1974). Thus, the clathrate hydrates are non-stoichiometric compounds (Davidson, 1973).

The Structure II hydrates have a 17 \AA cubic unit cell and contain 136 water molecules with 8 large cages (hexakaidecahedra which are 16 sided polyhedron) and 16 smaller cages (pentagonal dodecahedra) (Mak and McMullan, 1965). The ideal formula is $X \cdot 17 \text{ H}_2\text{O}$ (where X represents one gas molecule) (Davidson, 1973).

The hydrates (both structure types) are cubic whereas water ice crystallizes in the hexagonal system. Davidson (1973) and Larson (1955) have compared hexagonal water ice and hydrate structures. In the water ice lattice each oxygen is surrounded by 4 other oxygen atoms each at a distance of 2.76 \AA ($\text{O}-\text{O}$ bond distance = 2.76 \AA). Each water molecule is coordinated to 4 others by hydrogen bonds. The $\text{O}-\text{O}-\text{O}$ angles in water ice are essentially tetrahedral (109°). In the hydrates, each water molecule is coordinated to 4 others by hydrogen bonds (as is the case in all forms of ice including the high pressure polymorphs). The average departure of the $\text{O}-\text{O}-\text{O}$ angles from the tetrahedral values of hexagonal ice is 3.7° and 3.0° in Structure I and II hydrates respectively. This is much less than in the high pressure forms of ice. The $\text{O}-\text{O}$ bond lengths in hydrates exceed those in hexagonal ice by only 1% and are comparable to the bond lengths in other forms of ice. Davidson (1973) concludes that hydrates are properly ices with the "guest" molecules playing only a stabilizing and space filling role.

The thermodynamic conditions required for stability make it unlikely that the clathrate hydrates naturally occur on the earth in any abundance (Davidson, 1973). However, natural occurrences of clathrate hydrates

have been reported. Miller (1969) has proposed the existence of air hydrate, $(N_2O_2) \cdot 6 H_2O$, in the Antarctic ice cover. Khoroshilov et al. (1970) and Makogon et al. (1971) have reported the discovery of fields of natural gas hydrate beneath the permafrost of Siberia. Miller (1974) has suggested the possibility of natural gas hydrate fields occurring in Northern Canada and Alaska. Stoll et al. (1971) have proposed methane hydrate as an explanation for anomalous sound adsorption in certain deep sea sediments.

The factors which prevent abundant natural occurrence of the clathrate hydrates on the earth do not apply to other parts of the solar system. It is likely that methane hydrate exists in abundance on Uranus, Neptune, Saturn, Jupiter, and on the moons of Saturn and Jupiter (Miller, 1961, 1974; Lewis, 1969). Miller (1961), Delsemme and Swings (1952), Delsemme and Wegener (1970), and Delsemme and Miller (1970) have suggested that hydrates of CO_2 , CH_4 , C_2H_6 , and of other molecules exist in the heads of comets. Miller and Smythe (1970) and Miller (1974) have shown that the temperature and pressure measurements of the Mariner missions to Mars are consistent with the occurrence of CO_2 hydrate in the Martian icecaps.

This paper presents new evidence for the occurrence of CO_2 hydrate on Mars and assesses the geological implications of that occurrence.

CO₂ CLATHRATE HYDRATE ON MARS:

A PRE-VIKING ASSESSMENT

CO₂ clathrate hydrate was first prepared by Wroblewski (1882a, b) and subsequently prepared and/or studied by: Villard (1894, 1897), Hempel and Seidel (1898), de Forcrand (1902), Bouzat and Azinieres (1924), Tamman and Krige (1925), Herreillers (1936), Wiebe and Gaddy (1940), Frost and Deaton (1946), Unruh and Katz (1949), von Stackelberg (1949), Claussen (1951c), von Stackelberg and Muller (1951), Cole (1952), Larson (1955), Miller (1952), Miller (1961), Takenouchi and Kennedy (1964, 1965), Miller and Smythe (1970), and Smythe (1975). Details of most of these studies have been reviewed by Larson (1955) and Takenouchi and Kennedy (1965).

CO₂ hydrate is a Structure I hydrate with an ideal formula of CO₂ · 5.75 H₂O. The actual formula is closer to CO₂ · 6 H₂O because of the non-100% occupancy of the cages (Takenouchi and Kennedy, 1965). CO₂ hydrate has the same appearance (Miller and Smythe, 1970) and infrared reflectance spectra (Smythe, 1975) as ice.

Miller (1961) was the first to consider the possibility of the clathrate hydrates occurring on Mars. He expanded the dissociation data for the CO₂ hydrate (as well as for other hydrates) through the temperature range 175-232 K. He presented the data by the equation:

$$\log_{10} P_{hy} (\text{atm}) = 1121.0/T + 5.1524,$$

where P_{hy} is the dissociation pressure for the CO₂ hydrate and T is the absolute temperature. Miller used a surface pressure for Mars of 91.2 mb with nitrogen as the major component along with some argon and 1.5×10^{-3} atm. of CO₂ (data from Urey, 1959). Miller assumed a polar temperature of

180 K. He concluded that the pressures available were not sufficient to form a mixed hydrate of CO_2 , argon, and nitrogen from hexagonal ice. However, he pointed out that if unstable forms of ice are available (e.g. cubic ice) a mixed hydrate might form at the pole due to the unstable ice form lowering the dissociation pressure. Miller also concluded that the direct formation of a mixed hydrate in the Martian atmosphere may be possible if metastable ice or water droplets were present.

Mariner 4, 6, and 7 along with more refined earth-based observations greatly increased the accuracy and quantity of information about Mars. One of the major findings was that the Martian atmosphere was primarily CO_2 with no more than 1% nitrogen (Mutch et al., 1976). Mariner 7 data refined the temperature and pressure for the Martian polar cap to 153 K (Neugebauer et al., 1969) and 6.5 mb (which essentially represents the partial pressure of CO_2) (Kliore et al., 1969).

Miller and Smythe (1970) extended the dissociation pressure data for CO_2 hydrate through the temperature range 193-152 K (Figure 3). The dissociation pressure of CO_2 hydrate (P_{hy}) as a function of absolute temperature (T) is expressed by the equation:

$$(1) \log_{10} P_{\text{hy}}(\text{mb}) = 10.5591 - (1338.4/T) - 6.585 \times 10^{-3} T.$$

The vapor pressure of solid CO_2 (P_{CO_2}) is expressed by the equation:

$$(2) \log_{10} P_{\text{CO}_2}(\text{mb}) = 11.3450 - (1470.2/T) - 4.1024 \times 10^{-3} T$$

(Miller and Smythe, 1970).

Using the Mariner 7 polar pressure of 6.5 mb and equation (1), Miller and Smythe determined that the temperature at which the dissociation

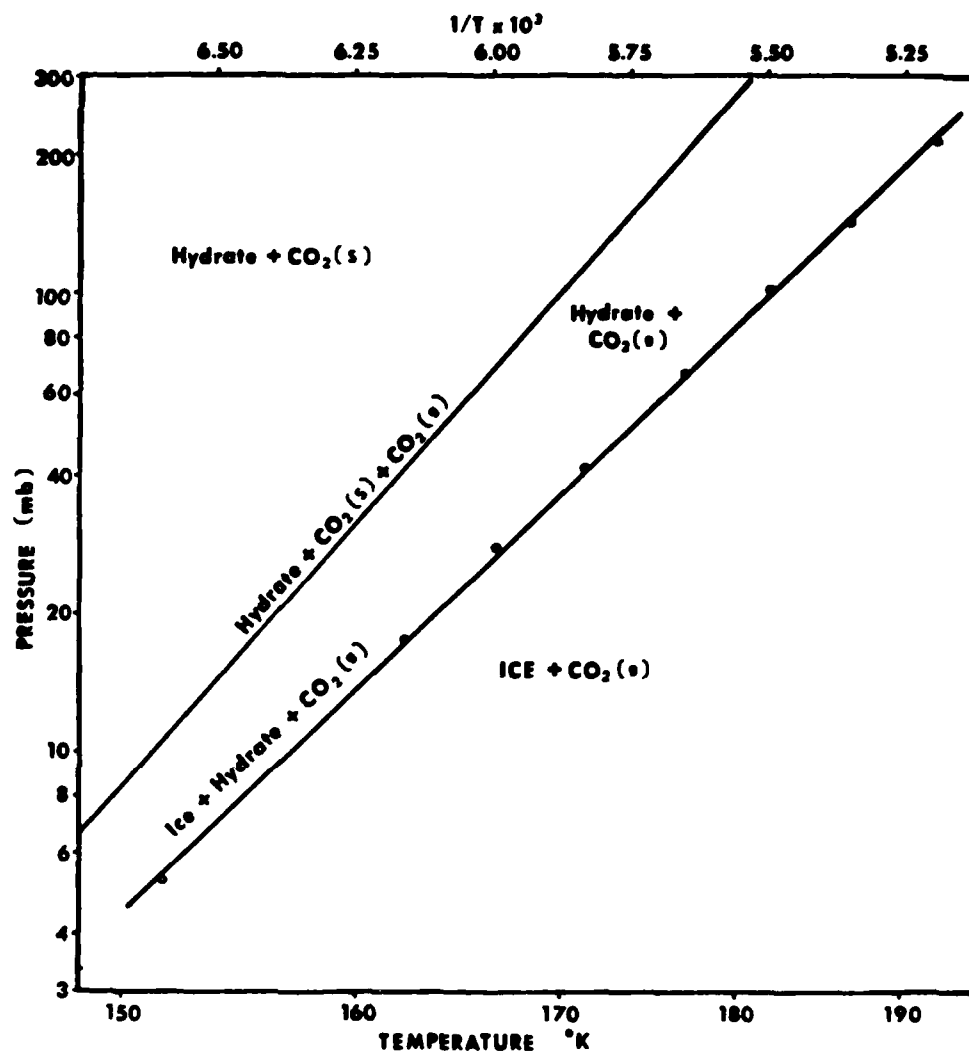


Figure 3. The dissociation pressure of CO₂ hydrate and the vapor pressure of solid CO₂. The circles are the experimental dissociation pressure measurements (After Miller and Smythe, 1970).

pressure of CO_2 hydrate is 6.5 mb is 153.18 K. This temperature is consistent with the polar temperature of 153 K obtained from Mariner 7 data. The stable phases of the $\text{CO}_2\text{-H}_2\text{O}$ system at 153 K are:

(1) at CO_2 pressures below 6.5 mb, ice and CO_2 (gas) are in equilibrium;

(2) at 6.5 mb, ice + CO_2 hydrate + CO_2 (gas) are in equilibrium;

(3) at CO_2 pressures between 6.5 and 13.1 mb, only CO_2 hydrate and CO_2 (gas) are in equilibrium;

(4) at 13.1 mb, only CO_2 hydrate + CO_2 (solid) + CO_2 (gas) are in equilibrium;

(5) above 13.1 mb, only CO_2 hydrate and CO_2 (solid) are present.

Miller and Smythe concluded that a Mars polar temperature of 153 K and a pressure of 6.5 mb could be accounted for on the basis of CO_2 hydrate in equilibrium with ice and CO_2 (gas). They also reported the following:

(1) above 121 K CO_2 hydrate is stable relative to CO_2 (solid) and water ice,

(2) the kinetics (rate of reaction) for the conversion of ice to CO_2 hydrate is critically dependent on the state of subdivision (particle size) of the ice,

(3) the conversion of finely divided ice to CO_2 hydrate at 150 K occurs in several hours.

Miller and Smythe point out that ice on Mars is likely to be very finely divided due to the small amount of water in the Martian atmosphere and

due to the absence of melting and refreezing. Thus:

(1) the Mars icecap can consist of water ice, water ice + CO_2 hydrate, or CO_2 hydrate + CO_2 (solid) depending on the temperature and pressure at any given time;

(2) the Mars icecap cannot consist of water ice + CO_2 (solid) without the presence of CO_2 hydrate;

(3) the formation of CO_2 hydrate in the Martian atmosphere is possible but because the amount of water vapor is so small the occurrence cannot be extensive.

Neugebauer et al. (1971) revised the polar temperature downward to 148 K at 6.5 mb and Herr and Pimentel (1969) reported spectroscopic evidence of CO_2 (solid). The temperature of 148 K and a pressure of 6.5 mb is consistent with the vapor pressure of CO_2 (solid) (Miller, 1974). Miller (1974) applied the revised temperature to the CO_2 hydrate case and pointed out that 148 K still leaves CO_2 hydrate stable but the phases in equilibrium are CO_2 hydrate + CO_2 (solid) + CO_2 (gas) rather than the previously proposed CO_2 hydrate + ice + CO_2 (gas) phases. Miller suggested that an equilibrium between the phases might not exist since the total conversion of the polar ice to CO_2 hydrate would be slow at 148 K unless the ice were very finely divided.

The revised Mariner 7 and Mariner 9 data indicated that both the southern and northern winter caps are at temperatures consistent with CO_2 (solid) (Kieffer et al., 1977). Independent spectroscopic evidence from Mariner 9 of the presence of CO_2 (solid) conclusively demonstrated that the seasonal polar caps are predominantly CO_2 (solid) (Herr and Pimentel, 1969; Kieffer et al., 1977). Cross (1971) calculates that at

maximum development the seasonal caps amount to 132 g cm^{-2} of CO_2 (solid) at the north pole and 164 g cm^{-2} at the south pole. Sharp (1974) calculates that the average thickness of the entire CO_2 (solid) blanket at both poles probably exceeds several centimeters.

Residual polar caps remain at both poles throughout the summer and are distinct from the thin seasonal mantles of CO_2 (solid) (Mutch et al., 1976). The data obtained through the Mariner 9 mission did not resolve the debate on the composition of the residual permanent caps (Kieffer et al., 1977). This debate centered around whether the residual caps were composed of water ice, CO_2 (solid), or a combination of the two (e.g., Ingersoll, 1974; Murray and Malin, 1973; Ward et al., 1974; Sagan et al., 1973; Briggs, 1974; Murray et al., 1972; Soderblom et al., 1973; Woiceshyn, 1974; Cross, 1971; Gierasch and Toon, 1973; Leovy, 1966; and Leighton and Murray, 1966).

Leighton and Murray (1966) predicted that the seasonal temperature changes at the Martian poles are small due to buffering by the vapor pressure of CO_2 in the atmosphere. During the autumn and winter the heat lost by the decrease in infrared radiation is supplied by the latent heat of condensation as the seasonal CO_2 (solid) cap grows. During the spring and summer the excess solar radiation over the outgoing infrared radiation goes into latent heat again as the seasonal cap retreats. These predictions were later supported by detailed observations of the polar caps (Murray et al., 1972; Soderblom et al., 1973; Herr and Pimentel, 1969; Neugebauer et al., 1969; Kliore et al., 1972; Chase et al., 1972).

If the residual polar caps are composed entirely of water ice (no permanent CO₂ solid), then the buffering effect would have to be accounted for by the CO₂ (solid) contained in the seasonal cap, which is only about 15% of the total CO₂ atmospheric content (Mutch et al., 1976). However, an effective natural solid buffer of a gas typically contains far more mass than is present in the gas phase (Fanale and Cannon, 1978). Therefore, if the seasonal CO₂ (solid) cap buffers the atmospheric pressure, the coincidence must exist that there has been just enough CO₂ supplied to the Martian surface to barely form the caps (Mutch et al., 1976). This small amount of CO₂ for the total outgassed quantity does not seem reasonable in view of the comparison of Mars with Earth and Venus. Ingersoll and Leovy (1971) report the ratio of the mass of CO₂ in the atmosphere to the mass of the planet is 4×10^{-10} for Earth, 4×10^{-8} for Mars, and 1.1×10^{-4} for Venus. The small value for Earth is acceptable by comparison because the earth has a known reservoir for its "missing" CO₂ in sedimentary rocks. The size of this reservoir indicates that the outgassing of CO₂ for the earth has been comparable to that for Venus (Ingersoll, 1974). This consistency of total outgassed CO₂ for Venus and Earth suggests that it might also be consistent for Mars. The abundance of Martian surface forms attributed to fluvial erosion is a strong indication that Mars indeed once had a more extensive atmosphere (Kieffer et al., 1976). If such an atmosphere once existed, the question of what happened to remove it has led to the hypothesis that there is a substantial reservoir of CO₂ on Mars.

Leighton and Murray (1966) proposed that there may be a reservoir of CO_2 (solid) at the residual icecaps that lasts throughout the year and is in vapor equilibrium with the atmosphere. Murray and Malin (1973) proposed a specific area of the northern residual ice cap as the location of a permanent reservoir of CO_2 (solid) averaging perhaps 1 km thick and containing 2-5 times the present Martian atmospheric mass.

Ingersoll (1974) summarizes the importance of the existence of a permanent reservoir of CO_2 (solid) as follows:

- (1) it would provide for a sink for storage of any CO_2 outgassed by Mars over geologic time in excess of the amount now in the atmosphere;
- (2) it would account for the atmospheric abundance of CO_2 simply as the vapor pressure of the solid reservoir;
- (3) it could, under proper orbital conditions, contribute to periodic reconstitution of a more dense atmosphere.

The main arguments against the existence of a permanent CO_2 (solid) reservoir are:

- (1) heating of the polar regions during the spring is too great to permit CO_2 (solid) to survive (Briggs, 1974);
- (2) the observed water vapor abundances in the atmosphere during the summer are much too high to be in equilibrium with a cold trap of CO_2 (solid) (Ingersoll, 1974).

Another explanation of the buffering of the atmospheric pressure has been offered. Fannale and Cannon (1971, 1974, 1978) have suggested

that the Martian regolith might contain a quantity of adsorbed CO_2 much greater than that present in the atmosphere-plus-cap system and might buffer that system and control its response to long term surface insolation change. However, Mutch et al. (1976) calculate that even under the best of conditions proposed by Fannale and Cannon (which they do not accept as correct), the amount of CO_2 that could be accommodated by the Martian regolith is only 5% of the amount that would be expected from a Mars that has outgassed as extensively as Earth.

Mutch et al. (1976) analyzed the possibility that exospheric escape of CO_2 (gas) could account for the lack of N_2 , H_2O , and CO_2 on Mars as compared to Earth. They conclude that exospheric escape may account for the lack of N_2 but it cannot account for the lack of H_2O (gas), or CO_2 (gas) (unless a mechanism existed for the removal of carbon in the form of CH_4). They account for the H_2O via a reservoir of permanent ground ice formed to depths of several kilometers. The CO_2 reservoir question is considered but no definitive answer is presented.

Dobrovolskis and Ingersoll (1975) propose CO_2 hydrate as a CO_2 reservoir on Mars. They used the equations of Miller and Smythe (1970) to determine that, for the Martian north and south poles, the temperature difference between the condensation of CO_2 (T_c) and the dissociation of CO_2 hydrate (T_d) is approximately 5 degrees Kelvin. In order to ascertain if the Martian icecaps could contain permanent CO_2 hydrate, they developed a complex model model to obtain the temperatures of the interior of the icecaps. The basis of the model is as follows:

(1) assumption that the icecaps were initially slabs of pure water ice;

(2) solutions of the one-dimensional heat diffusion equation to an accuracy of 1K;

(3) icecap heat exchange by:

- a. conduction in the interior,
- b. solar and atmospheric heating of the surface,
- c. infrared emission from the surface,
- d. latent heat exchange due to hydrate,

formation in the interior as well as by CO_2 condensation at the surface;

(4) use of a range of densities and thermal conductivities of the icecap (from that of solid ice to that of very fine snow);

(5) limitation of the rate of formation of hydrate from very fast (compared to a season) to very slow (compared to many years).

Consideration of all these factors varied the interior temperature by only a few degrees. Therefore, a simpler model was developed which yielded results within the range of those obtained with the more complex model.

The basis of the simpler model is that if heat exchange by conduction is neglected (as it is small even for solid ice) the temperature of the surface of a slab of ice at either pole at every moment is determined by equilibrium among:

- (1) the insolation,
- (2) advective atmospheric heating,
- (3) infrared cooling,
- (4) heat exchange due to the condensation and sublimation

of CO_2 .

Thus by keeping track of insolation and the rate of CO_2 condensation (and sublimation) the surface temperature of the icecaps can be determined as a function of season. Because the thermal skin depth is only a few meters at most, heat exchange from the surface condensation (and sublimation) of CO_2 and from the near surface (and surface) formation and (dissociation) of CO_2 hydrate is negligible. Therefore, the temperature of the interior of the icecaps must simply be the time average of the surface temperature over a year.

T_c and T_d for the north pole is (from Miller and Smythe's equations) 148.0 K and 153.2 K and 144.8 K and 149.1 K for the south pole. T_d represents an albedo of 0.65 for the north pole and 0.69 for the south pole. Dobrovolskis and Ingersoll conclude that these albedos are much more consistent with models of the Martian polar heat balance than the 0.71 or 0.74 albedo required by a permanent reservoir of CO_2 (solid). Therefore, they conclude that the icecap interior temperatures are between T_c and T_d and a CO_2 hydrate reservoir is probable. Moreover, a permanent reservoir of CO_2 hydrate, at least at the north pole, is consistent with Briggs' (1974) model of the seasonal polar caps. Further, CO_2 hydrate dissociation and formation on a seasonal basis is consistent with observed humidities while a permanent reservoir of CO_2 (solid) is not. The model predicts that the peak surface temperature achieved during the summer by a reservoir of CO_2 hydrate is about 200 K with some areas slightly warmer.

Ward (1974) and Ward et al. (1974) demonstrated that the obliquity of Mars varies considerably due to planetary perturbations with a period

of about 1.2×10^5 years. As a result, insolation of the poles can vary by as much as 40%. Ward et al. (1974) determined that if a permanent reservoir of CO_2 (solid) exists at the north pole, the obliquity variance can vary the polar temperature from 135.2K to 165.7K and the pressure consequently would vary from 0.65 mb to 25 mb. However, these calculations neglect atmospheric heating at the poles, which would lead to increased temperatures and therefore increase atmospheric heating and a runaway (positive feedback) situation (Dobrovolskis and Ingersoll, 1975). Thus, a reservoir of CO_2 (solid) would be unstable during periods of high obliquity and would release up to 1000 mb of CO_2 which would result in atmospheric instability (Sagan et al., 1973). Gierasch and Toon (1973) report that while a CO_2 (solid) reservoir would be unstable during the periods of high obliquity, CO_2 hydrate would be stable and only some tens of millibars would be added to the atmosphere. Dobrovolskis and Ingersoll calculate that the maximum pressure increase would be about 15 mb if the entire CO_2 hydrate reservoir dissociated.

Dobrovolskis and Ingersoll conclude that the mean temperatures of the polar caps are several degrees too high for the caps to contain permanent CO_2 (solid). They conclude that large amounts of CO_2 hydrate at the icecaps are consistent with observational data and with models of polar heat balance. They calculate that the polar caps may contain several millibars of CO_2 in the form of CO_2 hydrate. They suggest that the hydrate is controlling the atmospheric pressure and stabilizing it against large variations.

Another role for CO₂ hydrate on Mars has been suggested by Milton (1974). The Mariner 9 discovery of huge channels in the equatorial zone, some as much as 40 km wide and hundreds of kilometers long, with such features as accordant junctures, teardrop-shaped islands, braided reaches, and meandering courses strongly suggest that the channels were formed by running water (Milton, 1973). The channels appear immature by comparison with river systems on Earth and resemble catastrophic flood channels such as the complex scablands of Washington (Milton, 1973; Baker, 1973). Milton (1974) pointed out that this apparent fluvial activity implies the following:

- (1) surface temperatures and atmospheric pressures allowed the stability or at least the persistence of liquid water on or near the surface at one or more epochs in Martian history;

- (2) a source for the water existed;

- (3) the catastrophic nature of the channels implies that a mechanism for generating and releasing water at a rate rarely matched on Earth has occurred repeatedly on Mars.

The previous discussion of variations in planetary temperature and pressure with variations in planetary obliquity might satisfy the first point. The sudden melting of buried ice deposits has been proposed as a possible solution to the second and third points (Milton, 1973; Sharp et al., 1971; Sharp, 1973). The mechanisms proposed for melting the buried ice are local heating and meteorite impact (McCauley et al., 1972; Maxwell et al., 1973).

Milton (1974) attempted to solve the problem of how such a buried ice deposit could be melted without an extraordinary external heat source. He proposed that a CO_2 hydrate deposit buried between a few hundred meters and one kilometer would be stabilized by lithostatic pressure. This would place the hydrate in the equilibrium zone of hydrate + CO_2 (gas), between the quadruple points, and above the univariant line water + hydrate + CO_2 (gas) (Figure 4). The corresponding temperatures then would be between 271.65 K and 283.15 K. Milton concludes that the sudden formation of a crevasse open at a steep slope would cause a rapid depressurization of the hydrate deposit and its dissociation into liquid water and CO_2 (gas). The sudden presence of the liquid and the evolution of the gas would weaken the rock so that fracturing, decompression, and hydrate dissociation would propagate into the slope. The physical separation of the water from the rock on a broad drainage front would result in catastrophic dewatering and the formation of the chaotic terrain and the large channels in a single event.

Peale et al. (1975) point out that the depth of the buried hydrate deposit and the temperatures proposed by Milton allow liquid water as a stable phase and eliminate the requirement for the source of the chaotic terrain and the channels to be buried ice or hydrate deposits. In addition, they point out that only about one-third of the available water could be tied up in CO_2 hydrate if the original $\text{H}_2\text{O}/\text{CO}_2$ ratio were similar to that on Earth. Thus, a far larger volume of water would already exist in liquid form and could be released by any meteorite impact or tectonic activity which ruptured the overlying permafrost.

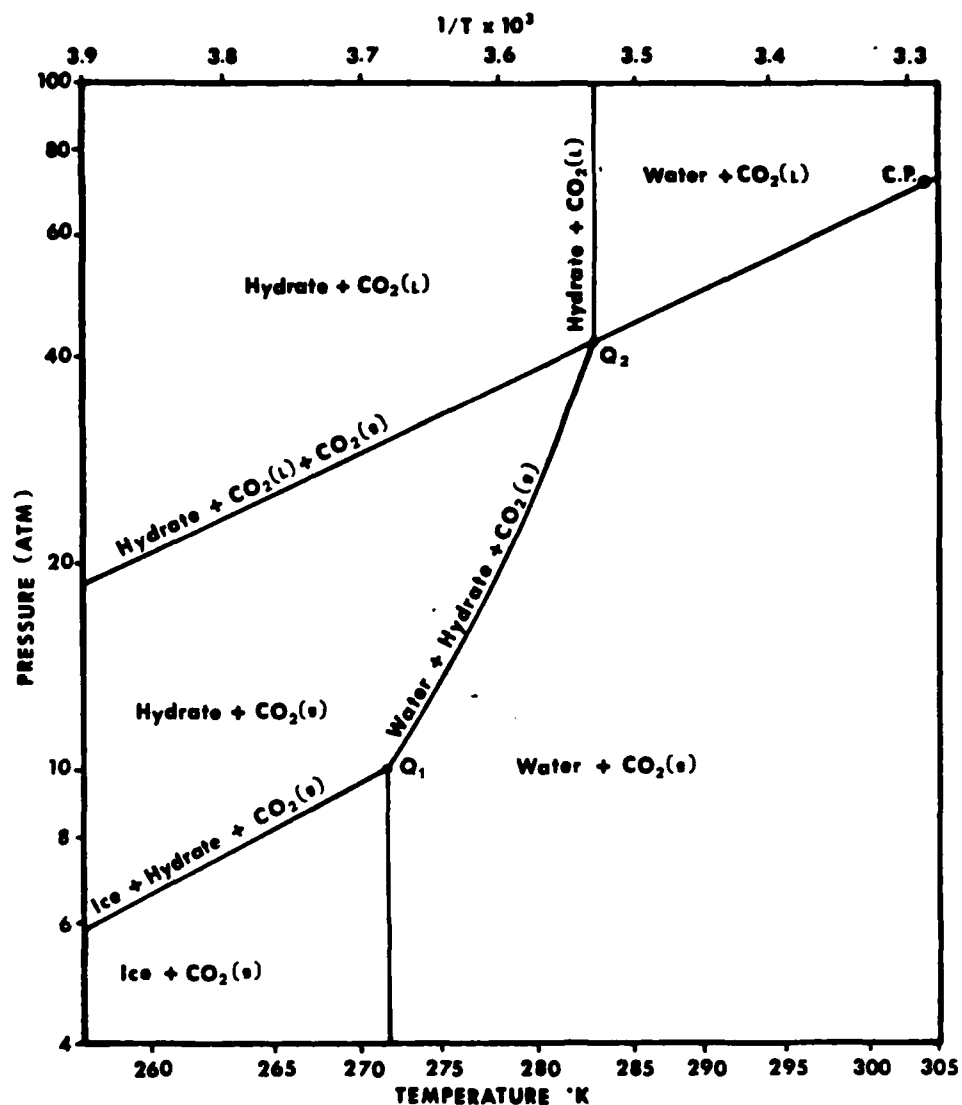


Fig. 4. The phase diagram of carbon dioxide hydrate near 273 K. C.P. is the critical point of carbon dioxide (304 K and 72.8 atm). Q₁ is the quadruple point [ice + water + hydrate + CO₂(g)] at 271.38 K¹ and 10.20 atm. Q₂ is the quadruple point [water + hydrate + CO₂(l) + CO₂(g)] at 283.35 K and 44.50 atm. (After Miller, 1974).²

Sharp (1974) suggests a much more limited role of CO_2 hydrate on Mars. He proposes that as winter approaches in the polar regions, a less than one millimeter (probably only a few micrometers) thick water-frost layer is deposited initially. (The thickness is limited severely by the low water-vapor content of the atmosphere). As temperatures approach 150 K the water frost layer converts to CO_2 hydrate. Although Sharp does not directly discuss the surface of the polar icecap converting to CO_2 hydrate, such a reaction is implicit in his scenario. The CO_2 hydrate would then be covered by CO_2 (solid) as the seasonal polar cap is deposited. The result would be a seasonal cap displaying vertical stratification with a very thin basal layer of CO_2 hydrate and a much thicker layer of CO_2 (solid) and any additional thin layers of CO_2 hydrate (if more water vapor could be condensed from the atmosphere). In addition, the seasonal cap would also display a concentric planimetric structure consisting of an outermost band (wide but thin) of water frost. Inside that band would be a narrower thin band of CO_2 hydrate. Finally, the central and largest layer would be CO_2 (solid). As the frost cover shrinks under rising temperatures the concentric banding also would shrink as the CO_2 hydrate converts to ice. Ultimately, water ice would be the last component.

Sharp points out that if there is a permanent body of CO_2 (solid) in the residual icecap then some CO_2 hydrate must also be present. Sharp does not include CO_2 hydrate as a factor in his discussion of ground ice on Mars.

The Mariner 9 mission discovered a set of apparent stacked layers in both the north and south polar regions. The individual layers are called lamina and the zones in which they appear, laminated (or layered) terrain. The total thickness of the layered terrain is approximately several kilometers and is comparable to the thickness of the residual polar caps (Sagan, 1973). The contrast in albedo of the layers and variations in surface texture suggests that the layered deposits are composed of different materials or different admixtures of the same materials (Sharp, 1974). The darker component is thought to be largely dust, volcanic ash, or both, and the lighter component may be frozen volatile materials condensed from the atmosphere (Murray and Malin, 1973). Sagan (1973) suggested that the volatiles probably are primarily CO_2 (solid) with ice and CO_2 hydrate as alternate candidates or co-existing phases. Sharp (1974) proposes two alternatives:

- (1) if the layered deposits accumulated under environmental conditions like those currently existing on Mars, the included volatile would be predominantly water ice;

- (2) if the layered deposits accumulated under conditions of colder temperatures, reduced solar radiation, or a denser atmosphere either CO_2 (solid), CO_2 hydrate, or both could be present. Sharp concludes that, because the layered deposits extend for at least twenty degrees from the poles, the principle volatile is water ice. However, he suggests that the included volatiles might show concentric zoning with a wide outer margin of water ice, an intermediate narrow zone of CO_2 hydrate, and a small central core of CO_2 (solid). Sharp

concludes that the included volume of volatiles is significant. If that volatile is ice, the amount included could exceed the amount of water present in the Martian atmosphere by an order of magnitude.

Finally, Mutch et al. (1976) conclude that a small amount of CO_2 hydrate may form in the polar areas but that the quantity is limited severely by the atmospheric water vapor content. They do not address the more likely method of CO_2 hydrate formation by direct conversion of the large amounts of ice present in the residual icecaps, layered terrain, and buried ice deposits.

In summary, the pre-Viking assessment of CO_2 hydrate occurrence offered a range from a small amount of CO_2 hydrate occurring to a large amount present as a reservoir controlling the Martian atmosphere. The geological roles suggested for CO_2 hydrate on Mars ranged from explaining the chaotic terrain and flood channels to no geological role.

A VIKING ASSESSMENT OF CO₂ HYDRATE OCCURRENCE ON MARS

The infrared thermal mapping experiment aboard the Viking orbiters measured surface temperatures of the northern residual ice cap of 205 K to 210 K (Kieffer et al., 1976). This is not in conflict with the summer surface temperatures predicted by Dobrovolskis and Ingersoll's (1975) model of the northern residual ice cap as a permanent body of CO₂ hydrate. However, Kieffer et al. conclude that the northern ice cap is composed entirely of water ice and water ice with dirt included. Kieffer and Palluconi (1979) conclude that the infrared thermal mapping and bolometric albedo data obtained by the Viking orbiters suggest that some solid CO₂ may survive the summer season at the residual southern ice cap. The southern permanent ice cap, then, also is a candidate CO₂ hydrate body. Thus, the data from the Viking orbiters have not eliminated CO₂ hydrate as a major component of the polar caps. Likewise the orbiter data have not confirmed the presence of CO₂ hydrate. However, the occurrence of condensate at the Viking Lander 2 (VL-2) site has provided the opportunity to determine if CO₂ hydrate occurs in the polar regions of Mars.

Jones et al. (1978) report that the first condensates began to form at the VL-2 site prior to sol 221 and accumulated at a nearly constant rate between sols 233 and 281. They report that initial accumulations formed on patches of fine-grained soil and later completely coated some small vesicular rocks. They conclude that the condensate was water ice because of its extremely slow sublimation rate and its persistence when

temperatures were approximately 20 K above the CO₂ frost point. Jones et al. believe that because of the small water vapor content in the atmosphere at the VL-2 site, the source for the water was the wetter equatorial region. They propose that water condensed onto dust particles suspended in the atmosphere above the equatorial region and were then transported by the atmosphere to the VL-2 area. The ice + dust particles were covered by CO₂ (solid) above the VL-2 site causing their precipitation to the surface. After precipitation, the CO₂ (solid) sublimated leaving a layer of ice and dust.

The proposal that ice coated dust particles were precipitated by CO₂ condensation on their surfaces suggests that the ice must have been exposed to temperatures consistent with CO₂ hydrate formation. However, investigation of CO₂ hydrate occurrence at the VL-2 site will be limited to the more easily quantifiable case of the deposited ice converting to hydrate.

The refined maximum and minimum temperatures at the VL-2 site for the period sol 232-310 along with the daily average pressure, the daily CO₂ hydrate conversion point (i.e., the temperature below which ice will convert to hydrate), and the daily CO₂ frost point are listed in Table 1 and shown in Figure 5. The maximum and minimum temperatures are from Ryan and Henry (1979). The daily CO₂ hydrate conversion point and CO₂ frost point were calculated using the daily average pressure and the equations of Miller and Smythe (1970) (see Fig. 3). The maximum standard deviation from the 24 hour mean pressure during any single sol was found to be 0.21 mb. This varies the CO₂ hydrate conversion point and CO₂ frost point by ± 0.2 K.

TABLE 1. Sol 232-310 data.

The refined daily maximum and minimum temperatures at the VL-2 site; the average daily pressure; the daily CO₂ hydrate conversion point; and the daily CO₂ frost point.

SOL	Minimum Temperature (°K)	Maximum Temperature (°K)	CO ₂ Hydrate Conversion Point (°K)	CO ₂ Frost Point (°K)	Average Pressure (mb)
232	151.0	162.7	156.8	151.0	9.81
233	155.5	166.0	156.8	151.0	9.81
234	156.0	168.0	156.8	151.0	9.80
235	153.3	168.2	156.9	151.1	9.94
236	155.0	167.0	156.9	151.1	9.89
237	156.0	169.0	156.8	151.0	9.80
238	151.0	159.0	156.7	150.9	9.68
239	152.0	163.0	156.9	151.1	9.94
240	154.1	172.0	156.9	151.1	9.94
241	154.6	166.2	156.8	151.0	9.78
242	153.1	161.8	157.0	151.2	9.95
243	154.0	164.0	157.0	151.2	10.02
244	153.0	166.0	156.9	151.1	9.89
245	155.0	162.6	156.9	151.1	9.89
246	154.1	161.5	157.0	151.2	9.95
247	155.6	164.0	156.9	151.0	9.77
248	153.7	163.5	156.6	150.9	9.62
249	153.1	164.9	156.8	151.0	9.78
250	153.4	163.6	156.9	151.1	9.87
251	154.9	161.0	156.8	151.0	9.82
252	154.0	161.2	156.8	151.0	9.76
253	152.3	161.6	156.9	151.1	9.90
254	154.1	162.0	156.9	151.1	9.87
255	153.0	159.0	156.7	150.9	9.74
256	152.3	160.5	156.9	151.1	9.94
257	154.0	162.0	156.9	151.1	9.92
258	152.7	162.7	157.0	151.2	9.97
259	151.0	165.0	156.8	151.0	9.79
260	152.6	159.1	156.9	151.1	9.92
261	156.0	172.0	156.9	151.1	9.85
262	151.0	163.5	156.7	150.9	9.70
263	154.9	159.0	156.8	151.0	9.83
264	155.0	163.6	156.9	151.1	9.85
265	155.0	162.3	156.8	151.0	9.82
266	154.3	163.9	156.8	151.0	9.84
267	153.8	158.8	156.8	151.0	9.81
268	154.0	163.0	156.8	151.0	9.80
269	157.0	168.0	156.7	150.9	9.74
270	151.7	158.4	156.6	150.9	9.56
271	153.9	159.0	156.7	150.9	9.70

TABLE 1 (Continued)

SOL	Minimum Temperature (°K)	Maximum Temperature (°K)	CO ₂ Hydrate Conversion Point (°K)	CO ₂ Frost Point (°K)	Average Pressure (mb)
272	153.9	161.0	156.7	150.9	9.67
273	154.1	158.8	156.6	150.9	9.58
274	150.9	157.0	156.8	151.0	9.81
275	152.7	157.4	157.0	151.2	9.97
276	153.8	158.8	157.1	151.2	10.12
277	155.4	161.7	157.1	151.2	10.12
278	158.7	164.0	157.0	151.2	10.04
279	161.1	166.2	156.9	151.1	9.91
280	159.2	161.4	156.9	151.1	9.89
281	155.7	159.3	156.9	151.1	9.89
282	154.9	158.2	157.0	151.2	9.97
283	153.6	157.1	157.0	151.2	9.98
284	154.3	157.3	157.1	151.2	10.14
285	154.0	158.5	157.2	151.3	10.16
286	155.1	160.4	157.1	151.2	10.09
287	155.3	158.8	157.1	151.2	10.05
288	155.1	158.4	157.0	151.2	10.04
289	154.6	159.1	157.0	151.2	10.02
290	154.3	157.4	157.0	151.2	10.04
291	154.0	157.6	157.1	151.2	10.11
292	154.3	158.1	157.1	151.2	10.09
293	153.9	157.8	157.1	151.2	10.07
294	153.5	156.8	157.0	151.2	10.01
295	151.6	157.8	157.0	151.2	9.99
296	154.6	158.7	157.0	151.2	10.02
297	153.4	158.7	157.0	151.2	10.03
298	153.9	158.9	157.0	151.2	10.04
299	153.8	158.9	157.0	151.2	9.98
300	154.1	159.7	157.0	151.2	9.90
301	153.4	158.8	156.8	151.0	9.84
302	151.2	158.2	156.9	151.1	9.88
303	151.1	158.0	156.9	151.1	9.89
304	151.5	158.2	156.9	151.1	9.88
305	151.1	159.8	156.8	151.0	9.80
306	153.7	161.5	156.8	151.0	9.79
307	153.7	158.6	156.9	151.1	9.85
308	151.4	158.4	156.8	151.0	9.84
309	151.3	159.5	156.8	151.0	9.81
310	150.4	158.7	156.8	151.0	9.82
Mean	153.8	161.4	156.9	151.1	9.89
Standard deviation of mean	1.9	3.6	.1	.1	.13

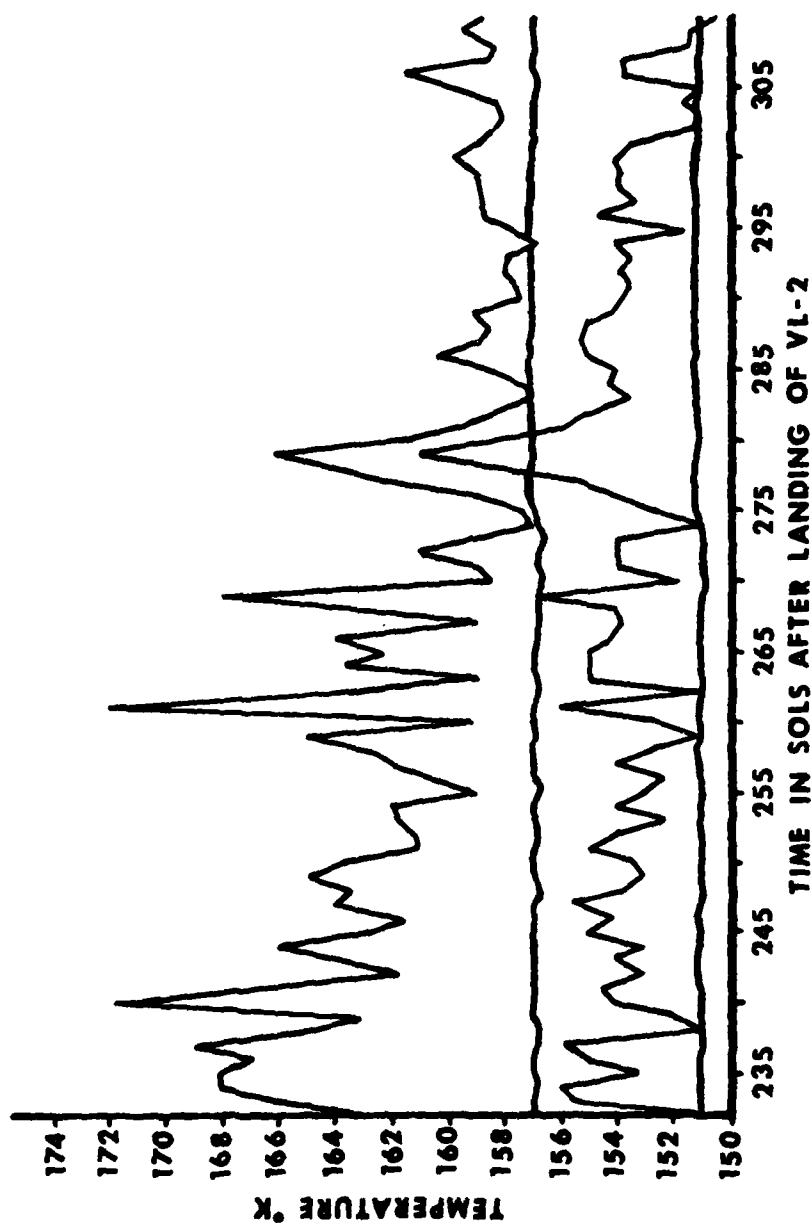


Figure 5. The maximum and minimum temperatures, CO_2 hydrate conversion point, and the CO_2 frost point for each sol during the period sol 232 to 310 at the VL-2 site.² The line at approximately 157 K indicates the daily CO_2 hydrate conversion point. The line at approximately 151 K indicates the daily CO_2 frost point. Maximum and minimum temperatures are from Ryan and Henry (1979).

As can be seen from Figure 5, the CO₂ hydrate conversion point was reached on every sol except sols 278, 279, and 280. From sol 232 to 310, the average CO₂ hydrate conversion point was 156.9 K \pm 0.1 K (see Table 1). The duration of temperatures below the CO₂ hydrate conversion point is difficult to determine for each sol because of the lack of refined data. Correction of the raw data independent of the principal investigators was not feasible. However, examination of Table 1 revealed that on several sols the maximum temperature barely exceeded the conversion point and on one sol, 294, the maximum temperature was below the conversion point. The pertinent data are presented in Table 2.

The temperature uncertainties are:

- (1) a refined temperature 2 sigma uncertainty of \pm 3.2 K (Hess et al., 1977; Ryan, 1979),
- (2) \pm 0.2 K uncertainty of the hydrate conversion point caused by using the sol average pressure in the calculation,
- (3) the uncertainty due to the lander temperature sensor location 1.6 meters above the surface (i.e., the surface would retain heat longer than the atmosphere).

If the uncertainty due to the location of the temperature sensor above the surface is neglected for the moment, then the worse case from the remaining uncertainties would increase the minimum and maximum temperatures in Table 2 by 3.2 K and lower the CO₂ hydrate conversion point by 0.2 K. This would result in only sols 274, 275, 294, and 295 still showing a minimum temperature below the conversion point. The maximum temperatures

TABLE 2. Sols on which the maximum temperature exceeded the CO₂ hydrate conversion point by less than 1 K.

SOL	Minimum Temperature (°K)	Maximum Temperature (°K)	CO ₂ Hydrate Conversion Point (°K)	Maximum Temperature Minus CO ₂ Hydrate Conversion Point (°K)
274	150.9	157.0	156.8	+0.2
275	152.7	157.4	157.0	+0.4
283	153.6	157.1	157.0	+0.1
284	154.3	157.3	157.1	+0.2
290	154.3	157.4	157.0	+0.4
291	154.0	157.6	157.1	+0.5
293	153.9	157.8	157.1	+0.7
294	153.5	156.8	157.0	-0.2
295	151.6	157.8	157.0	+0.8

would exceed the conversion point by 3.8 K, 3.8 K, 3.2 K, 3.2 K for sols 274, 275, 294, 295 respectively. However, the following points moderate this worse case:

(1) The use of the 2 sigma uncertainty still allows minimum and maximum temperatures below and only slightly above the conversion point. The actual refined temperature uncertainty is more likely 1 to 2 degrees kelvin (Ryan, 1979; Hess et al., 1977).

(2) The worse case still shows two cases of consecutive sols with minimum temperatures below the conversion point and maximum temperatures only a few degrees above the conversion point. This strongly indicates that the actual temperatures were consistent with the conversion of the ice to hydrate. Moreover, the fact that the temperatures prevailed for consecutive sols strongly indicates that the duration of temperatures below the conversion point was for a major portion of the two consecutive sols.

The uncertainty due to the location of the temperature sensor above the surface remains to be evaluated. Hess et al. (1977) report that the planetary surface brightness temperatures taken from Kieffer (1976) differ only slightly from the minimum air temperatures (5 K maximum) during the primary Viking mission (sol 0-60). Kieffer (1976) used the surface brightness temperatures to calculate that CO_2 frost would form at night at the VL-2 site during midwinter but would not last through the day. In addition, Jones et al. (1978) report a correspondence among minimum temperatures, maximum pressures, and the stability range of CO_2 solid at the VL-2 site from sol 220 to 320. They conclude that the CO_2 frost

point was indeed reached in the atmosphere at the height of the temperature sensors. They suggest that the consistency of the minimum temperatures indicates a buffering effect on the atmospheric temperature caused by the condensation of CO_2 on the surface. It would then seem reasonable to assume that the minimum temperatures listed in Tables 1 and 2 are very close to being correct and that the CO_2 frost point was reached at the surface on numerous occasions. Consequently, it is reasonable to conclude that the minimum temperatures were consistently well below the CO_2 hydrate conversion point.

Hess et al. (1977) report that the surface brightness temperatures of Kieffer (1976) differ by as much as 15 K warmer from the maximum air temperatures during the Viking primary mission. However, Jones et al. (1978), Ryan (1979), and Henry (1979) report that the dust storm activity over the VL-2 site resulted in continuous dust particle suspension in the atmosphere during sol 220 to 320. These particles lowered the effectiveness of the solar radiative heating of the surface (decreased insolation) and increased atmospheric heating resulting in a more consistent temperature for the air and surface (Jones et al., 1978; Ryan, 1979). Ryan (1979) estimates that the maximum air temperatures reported in Tables 1 and 2 are different from the surface temperatures by between 3 and 5 degrees Kelvin. In light of the analysis of the uncertainties of the temperature data, it remains probable that temperatures below the hydrate conversion point persisted repeatedly for significant lengths of time at the VL-2 site. However, it remains clear that the duration below the conversion point cannot be determined

quantitatively at this time. Therefore, the determination of the feasibility of conversion of the ice to CO_2 hydrate at the VL-2 site must be based on the time required for the conversion (rate of the reaction) and its compatibility with the temperature data presented thus far.

Miller and Smythe (1970) determined that the conversion of finely ground ice to CO_2 hydrate follows first order kinetics with rate constants of 0.22, 0.71, 1.4, and 2.2 hour^{-1} at 152, 162, 167, and 172 K respectively. They report that water condensed from the air at 78 K forms hydrate more rapidly than finely ground ice however, no rate constant was reported for this case. The nature of the ice at the VL-2 site is not known. The conditions of low atmospheric water content and the Jones et al. (1978) proposed method of accumulating the ice at the VL-2 site are not inconsistent with the assumption that the nature of the ice is somewhere between the finely ground ice used by Miller and Smythe and ice formed by condensing water from air at 78 K. Thus, the slowest rate of hydrate formation at the VL-2 site would be that represented by the data of Miller and Smythe and the fastest rate of formation would be that of the conversion of ice formed by condensing water from air at 78 K. Therefore, a rate constant was determined experimentally for the latter case.

The apparatus used consisted of a vacuum line, a temperature controlled reaction chamber, a CO_2 gas storage bulb, a transfer bulb, and a mercury manometer observed through a cathetometer (see Appendix 1). The

pressure measurement accuracy of the system was ± 0.1 mm Hg. The following procedure was used:

- (1) approximately 5 grams of distilled water were frozen in the transfer bulb,
- (2) the transfer bulb and the reaction chamber were then evacuated to 5×10^{-3} mm Hg,
- (3) approximately 2 grams of ice were vapor transferred into the reaction chamber whose base was just touching the surface of liquid nitrogen,
- (4) half of the reaction chamber was then submersed in liquid nitrogen,
- (5) the bottom of the chamber was then stabilized at 156 K,
- (6) CO_2 gas was then added until a pressure of approximately 9-10 mm Hg was established,
- (7) the change in pressure with time was observed as the ice converted to hydrate.

The experiment was performed twice. The initial pressure for Experiment 1 was about 1 mm Hg lower than that for Experiment 2. However, the rate of CO_2 adsorption was the same (within the uncertainty of the method) for both experiments. The pressure variation with time is shown in Figure 6. The initial pressure, the temperature variation with time, and the change in pressure with time are presented in Table 3. In addition, the rate constants calculated for each pressure measurement are presented along with the mean rate constant and standard deviation of the mean.

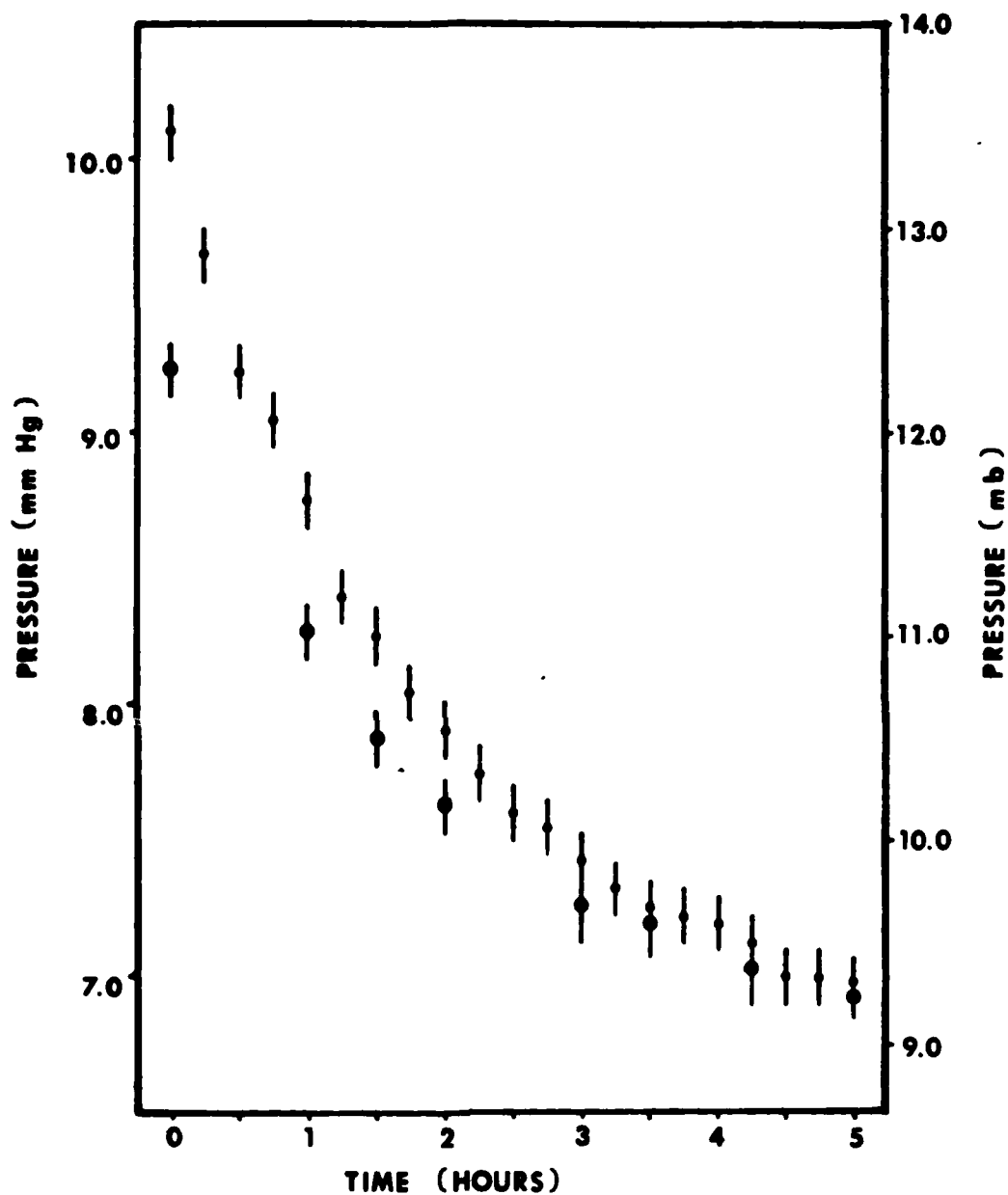


Figure 6. Change in CO₂ pressure with time as ice formed by condensing water from the air at 78° K is converted to CO₂ hydrate. Large dots are data from Experiment 1. Small dots are data from Experiment 2. Vertical lines indicate pressure uncertainty.

TABLE 3

DATA FROM EXPERIMENT 1:

TIME SINCE START		TEMPERATURE	PRESSURE	COMPUTED RATE
Hour	Minutes	(°K)	(mm Hg)	CONSTANT (k)
0	0	155.15	9.23	-
	5	155.65		
	10	156.15		
.25	15	156.49		
	20	156.49		
	25	156.49		
.50	30	155.65		
	35	155.65		
	40	156.15		
.75	45	156.49		
	50	156.82		
	55	156.49		
1.00	60	156.15	8.27	.50
	65	156.15		
	70	156.15		
1.25	75	156.49		
	80	156.82		
	85	155.65		
1.50	90	155.15	7.86	.55
	95	155.15		
	100	155.65		
1.75	105	156.15		
	110	156.49		
	115	156.82		
2.00	120	156.82	7.63	.54
	125	155.65		
	130	155.65		
2.25	135	156.15		
	140	156.15		
	145	155.65		
2.50	150	155.15		
	155	155.65		
	160	156.82		
2.75	165	156.49		
	170	155.65		
	175	155.15		
3.00	180	155.65	7.26	.55
	185	156.15		
	190	156.15		
3.25	195	156.15		
	200	155.15		
	205	156.82		
3.50	210	156.49	7.22	.50
	215	156.49		
	220	156.15		
3.75	225	156.15		
	230	156.15		
	235	155.15		
4.00	240	155.65		

TABLE 3 (Continued)

DATA FROM EXPERIMENT 1 (Continued):

TIME SINCE START		TEMPERATURE (°K)	PRESSURE (mm Hg)	COMPUTED RATE CONSTANT (k)
Hour	Minutes			
	245	155.65		
	250	155.65		
4.25	255	156.15	7.02	.57
	260	156.15		
	265	156.15		
4.50	270	156.82		
	275	156.82		
	280	156.49		
4.75	285	155.65		
	290	156.15		
	295	156.15		
5.00	300	156.15	6.94	.57
MEAN		156.06	-	.54
STANDARD DEVIATION OF THE MEAN		.50	-	.03

DATA FROM EXPERIMENT 2:

TIME SINCE START		TEMPERATURE (°K)	PRESSURE (mm Hg)	COMPUTED RATE CONSTANT k (hour ⁻¹)
Hour	Minutes			
0	0	155.65	10.10	
	5	156.15		
	10	156.49		
.25	15	155.65	9.65	.59
	20	156.49		
	25	156.15		
.50	30	155.65	9.22	.62
	35	155.65		
	40	156.49		
.75	45	156.49	9.05	.51
	50	156.15		
	55	156.49		
1.00	60	156.15	8.75	.53
	65	155.65		
	70	155.15		
1.25	75	156.15	8.40	.58
	80	156.15		
	85	155.65		
1.50	90	155.65	8.25	.55
	95	155.65		
	100	156.49		

TABLE 3 (Continued)

DATA FROM EXPERIMENT 2 (Continued):

TIME SINCE START Hour Minutes		TEMPERATURE (°K)	PRESSURE (mm Hg)	COMPUTED RATE CONSTANT k (hour ⁻¹)
1.75	105	156.15	8.05	.55
	110	156.15		
	115	155.65		
2.00	120	156.15	7.91	.54
	125	156.15		
	130	156.15		
2.25	135	156.15	7.75	.55
	140	156.49		
	145	155.65		
2.50	150	156.49	7.60	.57
	155	156.15		
	160	156.49		
2.75	165	155.65	7.55	.54
	170	156.15		
	175	156.49		
3.00	180	156.15	7.42	.56
	185	156.15		
	190	156.15		
3.25	195	155.65	7.33	.56
	200	156.15		
	205	156.49		
3.50	210	156.15	7.25	.57
	215	156.15		
	220	156.49		
3.75	225	156.82	7.24	.54
	230	155.65		
	235	156.49		
4.00	240	156.49	7.20	.53
	245	155.15		
	250	156.49		
4.25	255	155.65	7.12	.55
	260	156.15		
	265	155.65		
4.50	270	156.49	7.00	.62
	275	155.65		
	280	156.15		
4.75	285	156.15	7.02	.57
	290	155.65		
	295	156.49		
5.00	300	156.49	6.98	.58
MEAN		156.09	-	.56
STANDARD DEVIATION OF THE MEAN		.38	-	.03

The rate constant was calculated after the method of Miller and Smythe. The equation used was:

$$\ln [(P_0 - P_{oo})/(P - P_{oo})] = kt$$

where P_0 is the initial pressure, P_{oo} is the equilibrium pressure computed for the average temperature of the experiment using the equation of Miller and Smythe (see Fig. 3), P is the pressure as a function of time, k is the first order rate constant, and t is time in hours. Thus, the rate constant was determined as $0.54 \pm .03 \text{ hour}^{-1}$ at $156.06 \text{ K} \pm .50 \text{ K}$ for Experiment 1 and $0.56 \pm .03 \text{ hour}^{-1}$ at $156.09 \text{ K} \pm .38 \text{ K}$ for Experiment 2. The difference between the two measurements is within the uncertainty of the method. These data points along with Miller and Smythe's rate constants (and a least squares fit to their data) are shown in Figure 7. The new data confirm the Miller and Smythe observation of a higher conversion rate for ice condensed from the air.

During the time period sol 232 to 310, the average CO_2 hydrate conversion point was $156.89 \text{ K} \pm 0.13 \text{ K}$ and the average minimum temperature was $153.84 \text{ K} \pm 1.88 \text{ K}$ (150.4 K being the lowest temperature for the time period). Therefore, in calculating the time required to convert ice at the VL-2 site to hydrate, the fastest rate constant used was 0.56 hour^{-1} at 156.1 K (from Experiment 2) and the slowest rate constant used was 0.22 hour^{-1} at 152 K (from Miller and Smythe's data).

The proposed method of accumulation, the low water vapor content of the atmosphere, and the photographic evidence suggests that even at its maximum, the ice at the VL-2 site probably did not exceed a few micrometers in thickness (Jones et al., 1978). Therefore, the reaction rate at the

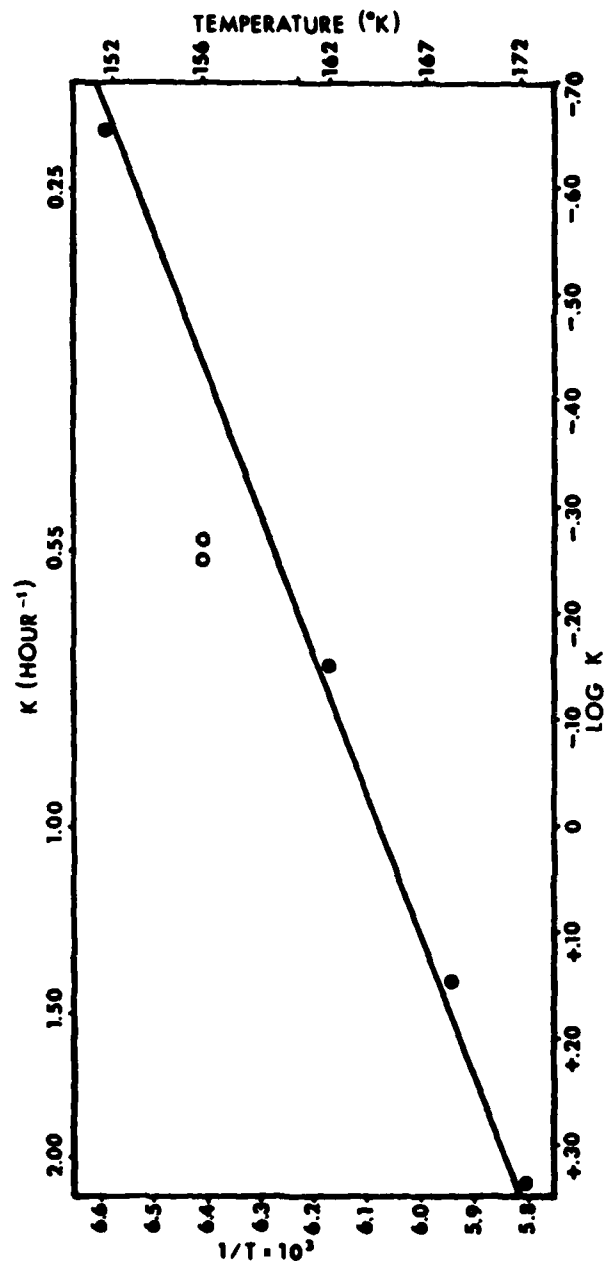


Figure 7. Experimentally determined rate constants for the conversion of ice to CO_2 hydrate. The dots indicate the rate constants for the conversion of finely ground ice to CO_2 hydrate (data from Miller and Smythe, 1970). The line indicates a least squares fit to Miller and Smythe's data. The circles indicate the rate constants for the conversion of ice formed by condensing water from air at 78°K (data from Experiments 1 and 2).

top and at the bottom of the ice layer can be assumed to be the same. The rate constants can, therefore, be applied directly and the time required to convert a percentage of the ice can be calculated from the following equation:

$$t = (1/k) \ln (100/100-x),$$

where t is the time required to convert x percent of the ice to hydrate given rate constant k . The results of the calculations are presented in Table 4.

Barrer and Ruzicka (1962) and Barrer and Edge (1967) report that conversion of ice to hydrate is a surface reaction with a hydrate layer forming on the surface of the ice preventing penetration of the gas and total conversion of the ice crystal. Therefore, it is reasonable to expect a maximum conversion of ice to hydrate at the VL-2 site of only 40 to 50 percent. A review of Table 4 shows that such a conversion will take place between 1 and 3 hours. A review of the minimum and maximum temperatures for the sols listed in Table 2 combined with the fact that the sols listed are in part consecutive allows the conclusion that 3 hours or more of temperatures below the hydrate conversion point is very probable. Therefore, it is concluded that there is a high probability that the ice at the VL-2 site converted to CO_2 hydrate at least on the sols listed in Table 2 and probably on numerous other sols as evidenced by the data listed in Table 1. Finally, the VL-2 location at 45°N latitude strongly indicates that higher latitudes provide conditions even more favorable for the conversion of ground ice to hydrate.

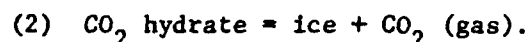
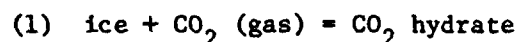
TABLE 4. The time (in hours) required to convert the VL-2 site ice to CO₂ hydrate.

PERCENT ICE CONVERTED	MINIMUM TIME REQUIRED (based on k of 0.56 hour ⁻¹ at 156.1 K)	MAXIMUM TIME REQUIRED (based on k of 0.22 hour ⁻¹ at 152.0 K)
10	0.19	0.48
20	0.40	1.01
30	0.64	1.62
40	0.91	2.32
50	1.24	3.15
60	1.64	4.16
70	2.15	5.47
80	2.87	7.32
90	4.11	10.47

GEOLOGICAL IMPLICATIONS OF
CO₂ HYDRATE OCCURRENCE ON MARS

Volume Changes of CO₂ Hydrate Formation and Dissociation

The occurrence of CO₂ hydrate on Mars could have geological implications due to the volume changes inherent to the reactions:



Dobrovolskis and Ingersoll (1975) calculated that ice expands by approximately 15% on conversion to CO₂ hydrate. They based their calculation on the unit cell dimensions of Structure 1 hydrate reported by von Stackelberg and Muller (1954). Von Stackelberg and Muller used x-ray unit cell dimensions of 12.00 Å and 12.12 Å to compute molar volumes of 22.6 cm³ and 23.3 cm³, respectively. They compared the hydrate molar volumes to the molar volume of ice (19.6 cm³). Thus, the conversion of one mole of ice to hydrate implied a volume expansion of 15.3% or 18.9% depending on the unit cell dimension used for the hydrate. Davidson (1973) reports that the unit cell dimensions for Structure 1 hydrates show no substantial dependence on the specific size of the encaged guest molecule. He reports that for guest molecules less than 5.5 Å in diameter all unit cell values are 12.03 ± 0.06 Å (5.5 Å diameter is the maximum size molecule that is known to form a structure 1 hydrate, see Fig. 1). Thus, the unit cell for CO₂ hydrate is 12.03 ± 0.06 Å and the molar volume is 22.80 ± 0.34 cm³. All unit cell dimensions cited were measured at 273.15 K (0°C). Therefore, the molar volume computed for CO₂ hydrate is for 273.15 K.

The molar volume of ice at 273.15 K is 19.65 cm^3 (calculated using a density of ice at 273.15 K of 0.91671 ± 0.00005 from Eisenberg and Kauzmann, 1969). Thus, the conversion of one mole of ice to CO_2 hydrate at 273.15 K causes a volume expansion of $16\% \pm 2\%$.

The molar volume of ice decreases as the temperature decreases. Based on the density of ice at various temperatures (obtained from x-ray data of LaPlaca and Post, 1960), the molar volume of ice decreases from 19.65 cm^3 at 273.15 K to 19.29 cm^3 at 93.15 K. However, the percent volume expansion resulting from the conversion of ice to hydrate can be assumed to remain constant over the temperature range because the primary component of hydrate is water and the primary bonding is the same as for ice.

An experiment was performed to measure the volume change when ice converts to CO_2 hydrate. The apparatus used consisted of a 50 ml. reaction bulb attached to a vacuum manifold by flexible tubing (see Appendix 2). The reaction bulb contained 250 one-eighth inch diameter steel ball bearings. The flexible tubing connecting the reaction bulb to the manifold allowed the bulb to be manually shaken. The agitation of the bulb caused the ball bearings to abraid the ice crystals in the bulb and maximize the formation rate of the hydrate (method from Barrer and Edge, 1967).

Because the objective of the experiment was to determine volume change, the volume of the apparatus had to be determined accurately. This involved determining the volume of the apparatus at different pressures and deriving a linear pressure-volume relationship (i.e., the change in pressure causes a change in the mercury level in the manometer and thus a change in the volume of the apparatus). The change in volume of the

apparatus with pressure was evaluated using the method described by Shriver (1969). That is, a known amount of CO₂ gas was transferred to the apparatus, the pressure and temperature measured, and the volume occupied by the gas calculated from the ideal gas equation:

$V = nRT/P$, where V = volume in cm³, n = moles, T = temperature (°K), P = pressure (mm Hg), and R is the gas constant (6.24×10^4 cm³ mm Hg/moles °K).

Table 5 presents the data obtained by the method.

TABLE 5. The change in volume of the apparatus with pressure.

TEMPERATURE (°K)	MOLES X 10 ⁻³ IN CHAMBER	PRESSURE (mm Hg)	CALCULATED VOLUME (cm ³)
294.33	0	0	-
295.39	1.01	87.25	213.37
294.33	3.08	262.07	215.85
294.29	3.11	264.54	215.89
294.59	4.35	367.88	217.36

A least squares fit to the data was computed as:

$$(1) \quad \text{Volume (cm}^3\text{)} = 1.42 \times 10^{-2} \times \text{Pressure} + 212.129.$$

The standard deviation of the slope and y-intercept were calculated as 7.01×10^{-5} and 0.018, respectively. The coefficient of determination was 0.99. The data are shown in Figure 8. The volume of the chamber

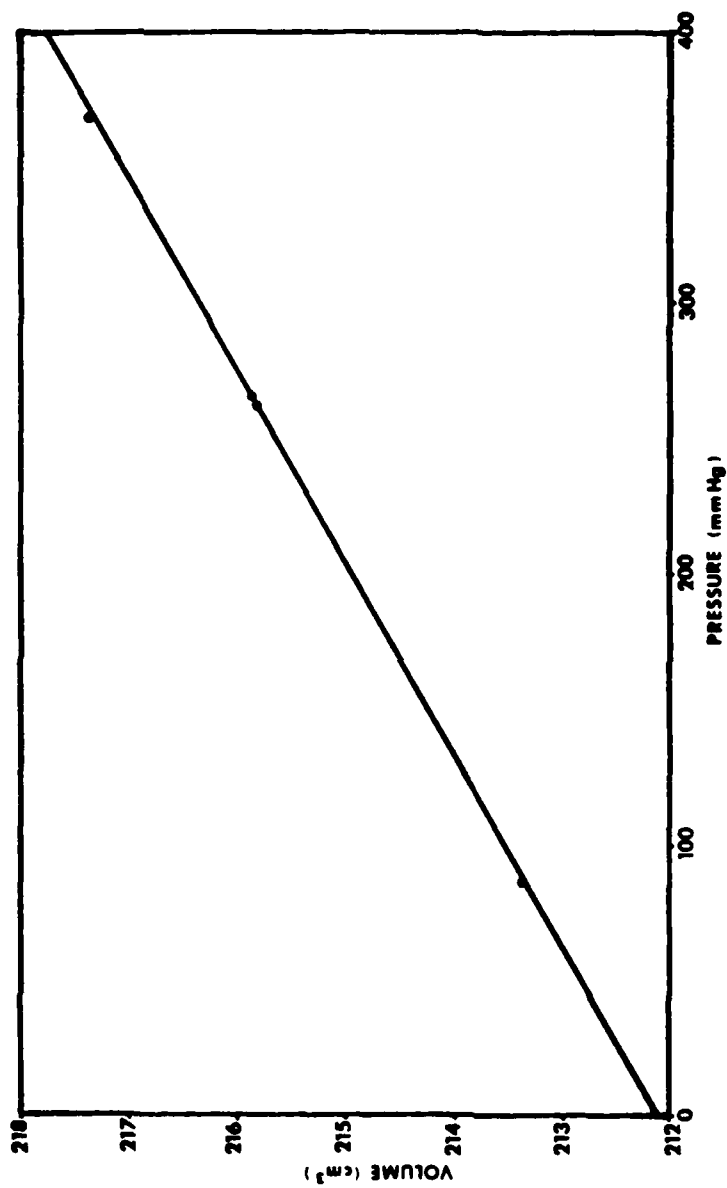


Figure 8. The volume-pressure relationship of the apparatus. Dots represent the calculated volumes listed in Table 6. The line represents a least squares fit to the data (see text, equation 1).

at zero pressure (actually 5×10^{-3} mm Hg) is the y-intercept of the least squares line and is $212.13 \pm 0.02 \text{ cm}^3$.

Because the experiment had to be done at low temperatures, and because the entire apparatus was too large to be temperature controlled, the ice to be converted to hydrate (in the reaction bulb) was held at a constant temperature and the gas allowed to obtain thermal equilibrium. However, for purposes of volume determinations, the temperature of the gas at thermal balance had to be established. Therefore, the procedure used to determine the volume of the apparatus was used to determine the temperature of the gas. The temperature selected for the experiment was dry ice temperature and an acetone-dry ice bath was used. The reaction bulb (containing only the ball bearings) was submersed in the bath. The temperature of the bulb was monitored by thermocouple sensors placed at the bottom and at the top (just below the acetone level). A known amount of CO_2 gas was added to the system. Fifteen minutes was allowed for the CO_2 to obtain thermal equilibrium. The pressure was monitored throughout the fifteen minute period and found to stabilize after 3.3 ± 0.1 minutes. The measured pressure was then used to calculate the volume occupied by the gas by equation (1). The gas temperature was then calculated from the ideal gas equation. The process was repeated a total of 6 times. The data are presented in Table 6. The gas temperature was found to be $211.78 \pm 0.61 \text{ K}$.

The experiment was then performed as follows. The reaction bulb was disconnected from the flexible tubing and placed in the acetone-dry ice bath. Finely divided ice was prepared by grinding the ice under liquid nitrogen with a mortar and pestle (method from Miller and Smythe, 1970).

Table 6. Calculated gas temperature at thermal equilibrium.

REACTION BULB TEMPERATURE (°K)	MOLES X 10 ⁻³ CHAMBER	IN	PRESSURE (mm Hg)	VOLUME FROM EQUATION (1) (cm ³)	CALCULATED TEMPERATURE (°K)
BOTTOM	TOP				
195.90	197.99	1.47	91.87	213.43	213.76
195.90	197.99	2.28	139.09	214.11	209.32
195.90	197.32	3.29	201.76	215.00	211.30
195.90	197.32	4.91	300.62	216.40	212.33
195.90	197.32	6.10	372.15	217.42	212.57
195.90	197.99	7.58	457.36	218.63	211.40
MEANS AND STANDARD DEVIATION OF MEANS					
195.90	197.66				211.78
	+ .15				+ .61

The ice was then transferred to the reaction bulb and the flexible tubing re-connected. The bulb was evacuated and the ice degassed by maintaining a vacuum of 5×10^{-3} mm Hg for 14 hours.

The addition of ice to the system changed the volume of the apparatus available to be occupied by gas. Values for this volume were determined as follows:

- (1) a known amount of CO_2 was added
- (2) the pressure was measured after 5 minutes
- (3) the measured pressure, the known amount of CO_2 added, and a gas temperature of 211.78 K were used to calculate the volume occupied by the gas (i.e., the volume not occupied by the ice).
- (4) the procedure was repeated for a total of three measurements.

Table 7 presents the data obtained by the method.

The reported dissociation pressure of CO_2 hydrate is 206.50 mm Hg at 196 K (Miller and Smythe, 1970). Analysis of the data presented in Table 7 shows that the bottom temperature (the temperature of the ice) was 196 K. Also, the data shows that the pressure required to form hydrate from ice (206.50 mm Hg) was not exceeded for the first two measurements but was exceeded for the third measurement. However, because the pressure measurements were made quickly after the addition of the CO_2 (within 5 to 7 minutes) and because the reaction rate for the conversion of ice to hydrate is small, the pressure measurement was not considered to have been significantly affected by hydrate formation. Similarly, adsorption of CO_2 by the degassed ice was not considered to have any measurable effect on the pressure measurement.

TABLE 7. The change in volume with pressure of the apparatus with ice in the reaction bulb.

TEMPERATURE OF REACTION BULB (°K)		MOLES X 10 ⁻³ ADDED	PRESSURE (mm Hg)	VOLUME CALCULATED ($V = \frac{nRT}{P}$, where $T = 211.78 \text{ K}$) cm ³
BOTTOM	TOP			
195.99	198.11	1.47	106.04	183.20
195.99	197.99	2.28	164.01	183.71
195.99	197.99	3.29	235.00	185.01

The hydrate was formed by adding known amounts of CO_2 and shaking the reaction bulb. The shaking was continued until the pressure approached equilibrium. Then, another known amount of CO_2 was added and the shaking continued. The procedure was repeated until the shaking of the bulb no longer resulted in a marked increase in the rate of reaction. The shaking was then stopped and the system was allowed to establish equilibrium. The equilibrium pressure was measured as 208.75 ± 0.14 mm Hg. This agrees within 1.1% with the 206.50 mm Hg pressure reported by Miller and Smythe (1970). It was assumed that, by allowing equilibrium to be obtained without shaking the bulb, all exposed ice surfaces converted to hydrate and a gas impenetrable barrier of hydrate coated each ice crystal. The barrier thus prevented further hydrate formation and allowed volume determination to be accomplished by adding CO_2 gas without concern over additional hydrate formation causing inaccurate pressure measurements.

If the conversion of the ice to hydrate resulted in a volume expansion, the volume of the apparatus available to be occupied by gas should be reduced from the volume available prior to the conversion. Values for the volume available to the gas were determined as follows:

- (1) the pressure was measured;
- (2) a known amount of CO_2 was added;
- (3) the pressure was measured after 5 minutes;
- (4) the pressure increase (ΔP) caused by the addition of the known amount of CO_2 was determined by subtracting the pressure measured in step (1) from the pressure measured in step (3);
- (5) ΔP , the known amount of CO_2 added, and a gas temperature of 211.78 K was then used to calculate the volume occupied by the added CO_2 ;

(6) the procedure was repeated for a total of three measurements.

Table 8 presents the data obtained by the method.

Comparison of the bulb temperatures (bottom and top) listed in Tables 6, 7, and 8 shows that the bottom temperature (temperature of the ice) remained very constant throughout the experiment. However, the data show that the top temperature varied but remained close to the top bulb temperatures measured during the measurement of the gas temperature (Table 6). Thus the gas temperature of 211.78 ± 0.61 K was considered usable. However, the uncertainty of the temperature (± 0.61 K) made it the largest source of error in the volume calculations. Figure 9 shows the calculated volume for each addition of CO_2 for both the ice and hydrate case. Error bars show the volume uncertainty caused by the ± 0.61 K temperature uncertainty.

Equation 1 shows that the volume change of the apparatus as a function of pressure (due to the mercury level changing in the manometer as the pressure changes) can be expressed as:

$$(1) \text{ Volume (cm}^3\text{)} = 1.42 \times 10^{-2} \times \text{Pressure} + 182.129.$$

The slope of the line (1.42×10^{-2}) is the expression of the change in volume with pressure. Therefore, regardless of the volume attached to the manometer, the slope of the volume-pressure line will remain constant at 1.42×10^{-2} . However, the y-intercept or volume at zero pressure (actually 5×10^{-3} mm Hg) will change if the volume attached to the manometer changes. Thus, when ice was added to the apparatus the volume at zero pressure was decreased (because the volume measured is the volume available for gas to occupy). And, when the ice converted to hydrate and expanded in

TABLE 8. The change in volume with pressure of the apparatus after the ice was converted to CO₂ hydrate.

TEMPERATURE OF REACTION BULB (°K)	MOLES X 10 ⁻³ ADDED	PRESSURE AFTER CO ₂ ADDED (mm Hg)	PRESSURE BEFORE CO ₂ ADDED (mm Hg)	PRESSURE DUE TO CO ₂ ADDED (ΔP)	VOLUME CALCULATED (V = nRT/P, where T = 211.78°K) cm ³
BOTTOM					
195.90	1.47	318.37	208.75	109.62	177.21
195.99	2.28	487.84	318.37	169.47	177.79
195.99	3.29	730.51	487.84	242.67	179.16
TOP					

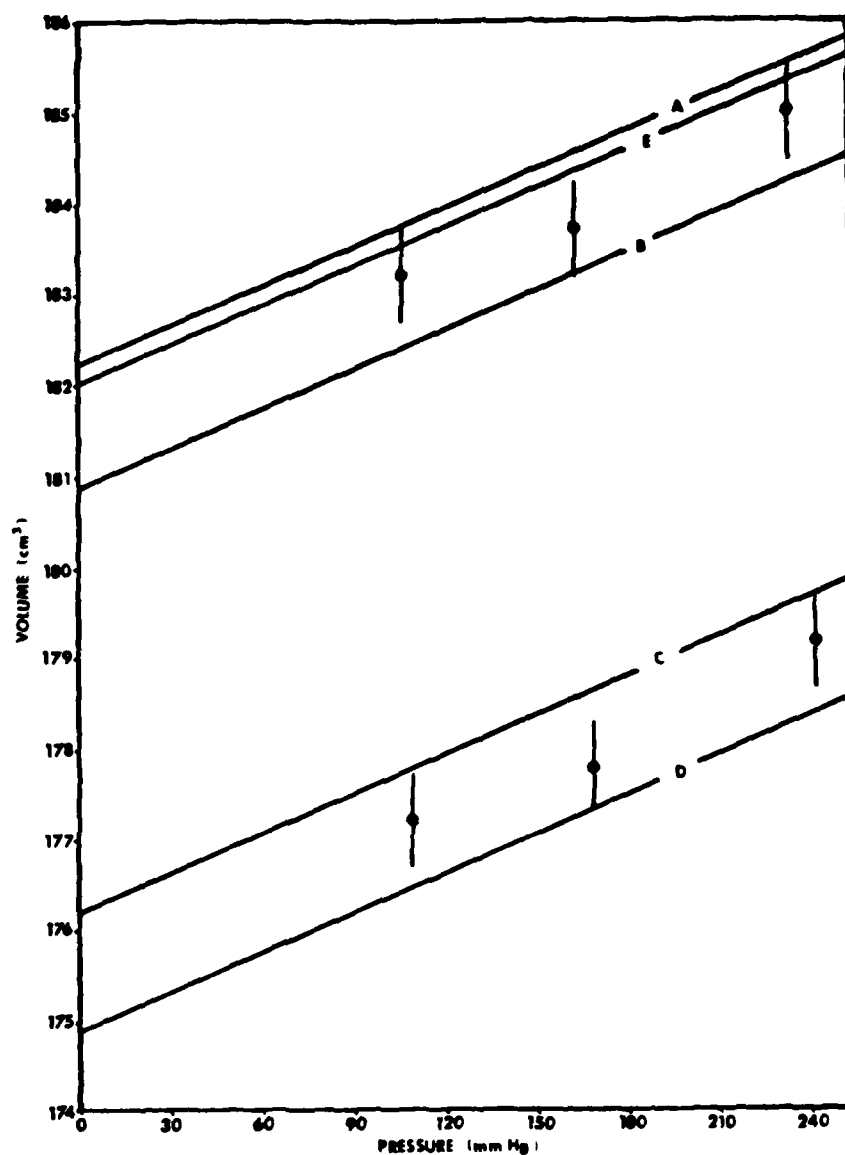


Figure 9. The volume-pressure measurements for the Ice and Hydrate cases. Dots represent calculated volumes listed in Tables 7 and 8. Vertical lines are volume error bars due to the uncertainty of the gas temperature. The y-intercepts of Lines A and B are the range of values for the volume at zero pressure for the ice case. The y-intercepts of Lines C and D are the range of values for the hydrate case. The y-intercept of Line E is the actual volume occupied by the ice determined by calculation after the experiment.

volume the volume at zero pressure was again reduced. Therefore, the volume occupied by the ice is equal to the volume at zero pressure before the ice was added (from equation 1, 212.13 cm^3) minus the volume at zero pressure after the ice was added. Similarly, the volume occupied by the hydrate (plus any unconverted ice) is equal to the volume at zero pressure before the ice was added (212.13 cm^3) minus the volume at zero pressure after the ice was added and converted to hydrate. However, due to the error bars caused by the temperature uncertainty specific volumes at zero pressure for the ice and hydrate cases cannot be determined. A range can be determined by constructing lines with slope of 1.42×10^{-2} at the limits of the error bars for each case. Lines A, B, C, and D of Figure 9 show the range of volumes at zero pressure for the ice case to be 182.22 cm^3 to 180.85 cm^3 . The range of volumes at zero pressure for the hydrate case is 176.23 cm^3 to 174.87 cm^3 .

To reduce the uncertainty, the amount of ice used in the experiment was measured after the experiment. That is, the ice was allowed to melt and the water weighed. The result was that $27.92377 \pm .00071$ grams or 1.55 moles of water were used. Using 196 K as the temperature of the ice during the experiment, a density of ice at 196 K of 0.9269 g cm^{-3} (from LaPlaca and Post, 1960), and a molar weight of water as 18.01534 grams, the molar volume of ice was calculated as 19.44 cm^3 . Therefore, the volume occupied by the 1.55 moles of ice used during the experiment was 30.13 cm^3 . Thus, the correct volume at zero pressure for the ice case is $212.13 - 30.13 = 182.00 \text{ cm}^3$. Using 182.00 cm^3 , a line of slope 1.42×10^{-2} is shown in Figure 9 (line E). This line lies between the lines constructed using the error bar limits for the ice case. Thus the 30.13 cm^3 volume

for the ice not only provides a unique volume for the ice case at zero pressure but also provides confidence in the experimental method.

The volume change from ice to hydrate can now be analyzed. The minimum volume expansion is 182.00 cm^3 minus the y-intercept for line C of Figure 9. That is, $182.00 - 176.23 = 5.77 \text{ cm}^3$. The maximum volume change is 182.00 cm^3 minus the y-intercept for line D of Figure 9. That is, $182.00 - 174.87 = 7.13 \text{ cm}^3$. The minimum percent volume expansion is $5.77 \text{ cm}^3 \times 100 / 30.13 \text{ cm}^3 = 19.15\%$. The maximum volume expansion is $7.13 \text{ cm}^3 \times 100 / 30.13 \text{ cm}^3 = 23.67\%$. These volume expansion percents must be related to the amount of hydrate formed before a percent expansion can be determined for the conversion of one mole of ice to hydrate.

During the experiment, the equilibrium pressure obtained was 208.75 mm Hg. The moles of CO_2 represented by this pressure depends on the volume occupied and the temperature of the gas. The gas temperature of $211.78 \pm 0.61 \text{ K}$ can be used. The volume occupied has the same range as the volume for the hydrate case (Figure 9, lines C and D). The equation for Line C of Figure 9 is $\text{Volume (cm}^3) = 1.42 \times 10^{-2} \times \text{Pressure} + 176.23$. The equation of Line D of Figure 9 is $\text{Volume (cm}^3) = 1.42 \times 10^{-2} \times \text{Pressure} + 174.87$. Thus, the range of volumes at a pressure of 208.75 mm Hg is 179.19 cm^3 to 177.81 cm^3 . The range of moles this pressure can represent is then (from the ideal gas equation using a gas temperature of 211.78°K) 2.83×10^{-3} to 2.81×10^{-3} . The amount of CO_2 added during the experiment was 2.14×10^{-1} moles. The amount of CO_2 adsorbed by the ice was 2.14×10^{-1} minus the moles of CO_2 required to give the 208.75 mm Hg equilibrium pressure (2.83×10^{-3} or 2.81×10^{-3} moles). The difference between 2.83×10^{-3} and 2.81×10^{-3} becomes negligible and the amount of CO_2 adsorbed is 2.11×10^{-1} moles.

Using a hydrate formula of $\text{CO}_2 \cdot 6\text{H}_2\text{O}$, 1.27 moles of ice were converted to hydrate. The volume expansion percentages calculated (19.15% minimum and 23.67% maximum) were for 1.27 moles of ice converted to hydrate. Expressed as a percent expansion for one mole of ice converted to hydrate, the minimum is $19.15\% \times 1 \text{ mole}/1.27 \text{ moles} = 15.8\%$. The maximum is $23.67\% \times 1 \text{ mole}/1.27 \text{ moles} = 18.64\%$. This range (15.8% to 18.64%) is in excellent agreement with the value of $16\% \pm 2\%$ obtained from x-ray unit cell dimensions at 273.15°K.

It is concluded that the percent volume expansion resulting from the conversion of one mole of ice to hydrate is $16\% \pm 2\%$. The dependence (if any) of percent expansion on temperature is within the uncertainty of the measurements. Conversely, when hydrate converts to ice a volume reduction occurs. The percent volume reduction (%VR) is given by:

$$\%VR = \frac{\text{change in volume as hydrate converts to ice}}{\text{Volume of hydrate}} \times 100.$$

$$\text{Substituting, } \%VR = \frac{16}{116} \times 100 = 13.79\%$$

Thus, when hydrate converts to ice on Mars, a volume reduction of approximately 14% occurs. If large bodies of ice convert to hydrate (or vice versa) on Mars, the volume changes accompanying the reactions should affect the geomorphology of the planet.

CO₂ Hydrate Dissociation and Martian Geomorphology

Carr and Schaber (1977) conclude that Mars' outgassing history and temperature conditions suggest that ground ice may occur to depths of several kilometers over large areas of the planet. Moreover, they find that the presence of ground ice is indicated by topographic features that resemble those found in periglacial regions on earth. One of these features, chaotic terrain, is defined by Carr and Schaber as a jumble of angular shaped blocks at a lower elevation than the surrounding terrain. They conclude that the formation mechanism was undermining and collapse. They point out that many large channels start in chaotic areas and that this suggests a genetic relationship between the two features.

The 14% volume reduction accompanying the conversion of CO₂ hydrate to ice may be an explanation for the chaotic terrain. The reduction would result in the collapse of the covering material. The associated channels could be caused by subsequent melting of the ice or by direct conversion of the hydrate to liquid water and CO₂ gas.

Sharp et al. (1971) and Sharp (1973) proposed that the sudden melting of a buried ice deposit would result in the formation of the chaotic terrain and a release of water at the rate required to create the associated channels. Milton (1974) attempted to solve the problem of how such a buried ice deposit could be melted without an extraordinary external heat source. He proposed that a buried hydrate deposit (stabilized by lithostatic pressure) could be rapidly depressurized by the sudden formation of a crevasse exposing the hydrate. The rapid depressurization would result in the dissociation of the hydrate into liquid water and CO₂ gas. Peale et al. (1975) showed that the depth of the hydrate deposit and the temperatures

proposed by Milton allowed liquid water as a stable phase and eliminated the requirement for the source of the chaotic terrain and associated channels to be buried ice or hydrate deposits. Depressurization of a hydrate deposit buried to depths less than proposed by Milton and/or at temperatures colder than proposed would result in the conversion of the hydrate to ice + CO₂ gas and no release of liquid water. Thus, it seems that an external heat source is required to cause the release of liquid water from either a buried ice or a buried hydrate deposit.

If the source for the chaotic terrain and its associated channels was the melting of a buried ice or hydrate deposit, then the amount of water required to create a specific channel is related to the dimensions of its chaotic terrain source area. The size of the chaotic terrain source area is, in turn, related to the volume vacated by the melted ice or hydrate deposit. A hydrate deposit would vacate a 16% larger volume and, consequently form a larger chaotic terrain area than an ice deposit containing the same amount of water. At present, the calculations of the amount of water required to create a Martian channel have not been linked with the dimensions of its chaotic source area. This is partly due to the lack of accurate depth data for the channels and partly due to the difficulty in estimating the volume decrease that caused the collapse of overlying material and the formation of the chaotic source area. Additional investigations and exploration of Mars may provide data allowing assessment of the amount of water required to form a channel and determination of its source as ice or hydrate.

CO₂ Hydrate Formation and Martian Geomorphology

It is not known how much ice may be deposited in any one area during the Martian winter. The ice deposition at the VL-2 site shows that at a minimum, enough ice is deposited to coat rocks (Jones et al., 1978). Perhaps enough is deposited to fill rock fractures and pore spaces. The maximum amount of ice that can be deposited is limited severely by the amount of water vapor in the Martian atmosphere and by the transport and accumulation processes. However, ground ice beneath and intermixed with the regolith is probably a larger and perennial source of ice. Carr and Schaber (1977) estimate that in some areas of Mars large proportions of ground ice (as much as 50%) may be dispersed throughout the host material. In addition, the layered terrain provides a source of ice in layers of ice and dust alternating with non-ice layers (Sharp, 1973). The volume expansion accompanying the conversion of these ice sources to hydrate may be of geological importance. Indeed, the polygonal-pattered ground in the region 40°-50°N latitude may have resulted from ice-wedging-like action (Carr and Schaber, 1977). This ice-wedging-like action may have been the conversion of ice to hydrate rather than the conversion of liquid water to ice. However, for the conversion process to cause mechanical weathering of rocks, ground heaving, polygonal-patterned ground, or other geologically significant events, the ice must convert to hydrate in at least partially confined spaces and the accompanying volume expansion must exert a force on the confining walls.

An experiment was performed in an attempt to measure the force that the conversion of ice to hydrate in a confined space exerts. The

apparatus used consisted of a chamber that could be maintained at 213 K for extended time periods, a CO₂ storage bulb, and a mercury manometer capable of indicating 2.5 atmospheres of pressure (see Appendix 3).

An axial (longitudinal) and a circumferential precision electrical resistance strain gauge, rated for low temperature performance on aluminum, (gage type EK-15-250BG-350W3 manufactured by Micro Measurements of Romulus, Michigan) were mounted according to manufacturer's specifications on a thin walled aluminum tube (tube dimensions: 2 cm outer diameter, 1.98 cm inner diameter, 13.5 cm long). The gauges and a thermocouple were wired through the removable vacuum electrical feedthrough used to seal the chamber. The strain gauge wires were connected to a digital strain indicator (DSI) through a switch and balance unit (SBU) (Model 201 DSI and Model 301 SBU manufactured by Bean Inc., Detroit, Michigan). The DSI measurement sensitivity is $\pm 1 \times 10^{-6}$ units of strain. Fifty pin hole size holes were drilled in the screw-on top of the aluminum tube to allow CO₂ flow into the tube.

The experiment was conducted as follows:

(1) Day zero (start of experiment): The axial and circumferential strain gauges on the empty aluminum tube were balanced to zero with the SBU. The empty tube was then placed in the chamber and a temperature of 213 K and a pressure of 5×10^{-3} mm Hg were established in the chamber.

(2) Day 1: The axial and circumferential strains were measured at -45×10^{-6} and -41×10^{-6} units of strain, respectively.

(3) Day 2: No change was found in the strain.

(4) Day 3: The strain measurements showed no change from the previous two days. The negative axial and circumferential strains were considered consistent with a temperature induced contraction of the aluminum tube. The axial and circumferential strains were balanced to zero with the SBU, to eliminate this effect.

(5) Day 3 to 24: Strains were recorded every 24 hours. No significant change was observed. Table 9 lists the strain data recorded for this first empty tube experiment.

(6) Day 24 (within 2 hours of Day 25): The tube was removed, the top taken off, and 12.5 cm of the tube's 13.5 cm length was submersed in liquid nitrogen. Finely divided ice, prepared by grinding ice under liquid nitrogen with a mortar and pestle, was then loaded in the tube. The ice was transferred to the tube and settled by manually shaking the tube. A maximum amount of ice was loaded in the tube by repeating the transfer and settling process until no further settling occurred. The top to the tube was then screwed on the tube.

(7) Day 25: The tube was removed from the liquid nitrogen and placed in the pre-cooled (to 213K) chamber). The ice was then degassed by maintaining a 5×10^{-3} mm Hg pressure in the chamber for the remainder of day 25. The axial strain and circumferential strain at the end of Day 25 was measured as -16×10^{-6} and $+17 \times 10^{-6}$ units of strain, respectively.

(8) Day 26: CO_2 gas was added until a pressure of 1757.50 mm Hg was established in the chamber. At the end of Day 26, 9.47% of the ice in the tube had converted to CO_2 hydrate (see Appendix 3 for the method of determining the percent ice converted to hydrate). The axial and circumferential strains were measured as -16×10^{-6} and $+16 \times 10^{-6}$

TABLE 9. Strain data recorded during the first empty tube experiment (Day 0 to Day 24).

DAY OF EXPERIMENT	APPARENT AXIAL STRAIN (X 10 ⁻⁶ units)	APPARENT CIRCUMFERENTIAL STRAIN (X 10 ⁻⁶ units)	CONDITIONS
0	0	0	At room temperature and pressure.
1	-45	-41	In chamber at 213 K and 5 X 10 ⁻³ mm Hg pressure.
2	-45	-41	"
3	0	0	Same conditions as Days 1 and 2 but strains balanced to zero.
4	0	+1	Same conditions as prior 3 days.
5	0	-1	"
6	+1	-1	"
7	-1	0	"
8	0	-1	"
9	0	-1	"
10	-1	-1	"
11	-1	-2	"
12	0	0	"
13	-1	0	"
14	0	-1	"
15	0	-1	"
16	0	0	"
17	0	-1	"
18	+1	0	"
19	0	0	"
20	0	0	"
21	0	+1	"
22	0	0	"
23	0	0	"
24	0	0	Tube removed from chamber after strains recorded.

units of strain, respectively.

(9) Day 27 to 52: Strain and pressure measurements were made at the end of each day.

(10) Day 53: The hydrate formed was dissociated into ice by condensing the CO_2 gas out of the chamber into the storage bulb. Dissociation to ice and degassing of the ice was assured by maintaining a pressure of 5×10^{-3} mm Hg in the chamber for the remainder of Day 53 (approximately 20 hours).

(11) Day 54: Accuracy of the strain data was tested by repeating the hydrate formation. CO_2 gas was added until a pressure of 1756.85 mm Hg pressure was established in the chamber. At the end of Day 54, 11.49% of the ice had converted to hydrate. The axial and circumferential strains were measured as -16×10^{-6} and -17×10^{-6} units of strain, respectively.

(12) Day 55 to 78: Strain and pressure measurements were made at the end of each day.

(13) Day 79: The hydrate formed was dissociated using the same procedure used on Day 53.

(14) Day 80: The chamber was opened and the tube removed. The ice was allowed to melt. The water was then removed and weighed. The amount of ice used in the experiment was found to be 8.93×10^{-1} moles. Table 10 presents the data obtained during the hydrate formation part of the experiment.

In order to separate the effects of hydrate formation from other effects on the strain measurements, a "control" experiment was performed. The control experiment essentially repeated the hydrate formation

TABLE 10. Data from the hydrate formation experiment. The tube was loaded with ice and placed in the chamber at 213 K. CO₂ was added and hydrate formation started on Day 26. The hydrate was dissociated on Day 53. A second hydrate formation period was started on Day 54. The hydrate was dissociated on Day 79. The experiment was concluded on Day 80 and the tube was removed from the chamber.

DAY OF EXPERIMENT	APPARENT AXIAL STRAIN (X 10 ⁻⁶ units)	APPARENT CIRCUMFERENTIAL STRAIN (X 10 ⁻⁶ units)	PERCENT ICE CONVERTED TO CO ₂ HYDRATE
25	-16	+17	0
26	-16	+16	9.47
27	-16	+15	13.03
28	-15	+12	15.52
29	-17	+11	17.21
30	no data recorded		
31	-15	0	19.48
32	-16	- 6	21.16
33	-16	-11	22.64
34	-16	-12	24.26
35	-16	-12	25.87
36	-16	-13	27.41
37	-16	-15	28.49
38	-16	-16	29.83
39	-16	-16	30.64
40	no data recorded		
41	-15	-16	32.25
42	-15	-20	33.39
43	-15	-20	34.27
44	-15	-20	34.94
45	no data recorded		
46	no data recorded		
47	no data recorded		
48	-12	-21	37.69
49	-11	-21	38.70
50	-11	-21	39.51
51	-12	-21	39.77
52	-12	-21	40.04
53	-16	-16	0
54	-16	-17	11.49
55	-15	-18	14.24
56	-16	-17	16.13
57	-17	-18	17.67
58	-16	-18	18.68
59	-17	-18	20.16

TABLE 10 (Continued)

DAY OF EXPERIMENT	APPARENT AXIAL STRAIN (X 10 ⁻⁶ units)	APPARENT CIRCUMBERENTIAL STRAIN (X 10 ⁻⁶ units)	PERCENT ICE CONVERTED TO CO ₂ HYDRATE
60	-17	-19	21.10
61	-17	-18	22.04
62	-17	-17	23.84
63	-18	-19	24.79
64	-17	-19	25.94
65	-17	-19	26.67
66	-17	-18	28.15
67	-17	-18	29.29
68	-17	-18	30.24
69	-17	-19	30.97
70	-16	-20	31.98
71	-14	-20	32.99
72	-15	-21	33.86
73	-15	-19	34.47
74	-12	-20	35.07
75	-14	-21	36.08
76	-13	-21	36.48
77	-12	-21	37.29
78	-12	-21	37.76
79	-16	-16	0

experiment except that the chamber pressure was obtained with argon gas rather than CO_2 gas. Because the pressure and temperature conditions of the experiment (213 K and 1750 mm Hg) were not consistent with the formation of argon gas hydrate, the ice in the tube did not convert to hydrate. Therefore, the strains measured were not caused by the expansion of ice converting to hydrate. At the conclusion of the experiment (Day 52), it was found that the quantity of ice used in the experiment was only slightly more than used in the hydrate formation experiment (8.93×10^{-1} moles as compared to 8.95×10^{-1} moles).

At the conclusion of the experiment, the empty tube was returned to the chamber and a pressure of 5×10^{-3} mm Hg maintained for 22 days (Day 52 to 73). Strains were measured at the end of each day. The axial direction showed a zero strain (the same as the first empty tube experiment) with a slight but negligible drift. The circumferential strain measured $+11 \times 10^{-6}$ units of strain with a slight but negligible drift. By comparison, the first empty tube experiment gave a circumferential strain of zero. This was indicative of a circumferential strain shift during the experiment (probably on day 12 of the control experiment) of $+11 \times 10^{-6}$ units of strain.

Table 11 presents the strain data during the control experiment. Table 12 presents the post-experiment empty tube strain data.

Figure 10 shows the percent ice converted to hydrate per day during the hydrate formation experiment (data listed in Table 10). Analysis of Figure 10 and knowledge that 8.93×10^{-1} moles of ice were used in the experiment allowed the following observations and conclusions:

- (1) The formation rate and percent ice converted to hydrate for the two hydrate formation periods was essentially the same. It was

TABLE 11. Strain data from the control experiment. The tube was loaded with ice and placed in the chamber at 213 K. Argon gas was added to a pressure equivalent to the CO₂ pressure used in the hydrate formation experiment. Conditions were inconsistent with the formation of argon gas hydrate. Therefore, the strains measured were the result of factors other than the conversion of ice to hydrate.

DAY OF EXPERIMENT	APPARENT AXIAL STRAIN (X 10 ⁻⁶ units)	APPARENT CIRCUMFERENTIAL STRAIN (X 10 ⁻⁶ units)	CHAMBER PRESSURE (mm Hg)
0	-14	+18	0
1	-15	+16	1756.70
2	-17	+15	1754.41
3	-16	+ 8	1754.42
4	no data recorded		
5	-15	+ 1	1754.40
6	-15	- 8	1754.40
7	-16	-12	1754.39
8	-16	-14	1754.41
9	-18	-16	1754.40
10	-18	-20	1754.40
11	-18	-19	1754.42
12	-18	-10	1754.44
13	-18	-14	1754.41
14	-17	-12	1754.42
15	-18	-14	1754.40
16	-18	-14	1754.43
17	-18	-15	1754.44
18	-18	-15	1754.40
19	-18	-16	1754.41
20	-18	-15	1754.44
21	-19	-15	1754.43
22	-18	-15	1754.40
23	-17	-15	1754.39
24	-18	-15	1754.40
25	-18	-15	0

TABLE 11 (Continued)

DAY OF EXPERIMENT	APPARENT AXIAL STRAIN ($\times 10^{-6}$ units)	APPARENT CIRCUMFERENTIAL STRAIN ($\times 10^{-6}$ units)	CHAMBER PRESSURE (mm Hg)
26	-13	-10	1752.30
27	-15	-16	1750.28
28	-16	-14	1750.28
29	-15	-16	1750.30
30	-16	-17	1750.31
31	-17	-16	1750.29
32	-16	-16	1750.29
33	-16	-16	1750.32
34	-17	-14	1750.30
35	-17	-15	1750.29
36	-17	-17	1750.31
37	-17	-16	1750.31
38	-17	-17	1750.29
39	-17	-17	1750.28
40	-18	-17	1750.30
41	-17	-17	1750.33
42	-17	-16	1750.28
43	-18	-16	1750.29
44	-17	-16	1750.28
45	-17	-16	1750.32
46	-17	-17	1750.32
47	-17	-15	1750.32
48	-17	-16	1750.33
49	-17	-16	1750.30
50	-17	-16	1750.30
51	-14	-11	0

TABLE 12. Post-experiment empty tube strain data.

DAY OF EXPERIMENT	APPARENT AXIAL STRAIN ($\times 10^{-6}$ units)	APPARENT CIRCUMFERENTIAL STRAIN ($\times 10^{-6}$ units)	CONDITIONS
52	- 1	+11	In chamber at 213 K and 5×10^{-3} mm Hg pressure
53	- 2	+10	"
54	0	+11	"
55	+ 1	+12	"
56	0	+11	"
57	0	+11	"
58	0	+12	"
59	0	+13	"
60	+ 1	+11	"
61	- 1	+11	"
62	0	+12	"
63	- 1	+11	"
64	- 1	+11	"
65	- 2	+11	"
66	0	+10	"
67	0	+10	"
68	0	+11	"
69	0	+10	"
70	- 1	+10	"
71	0	+11	"
72	0	+11	"
73	0	+10	"

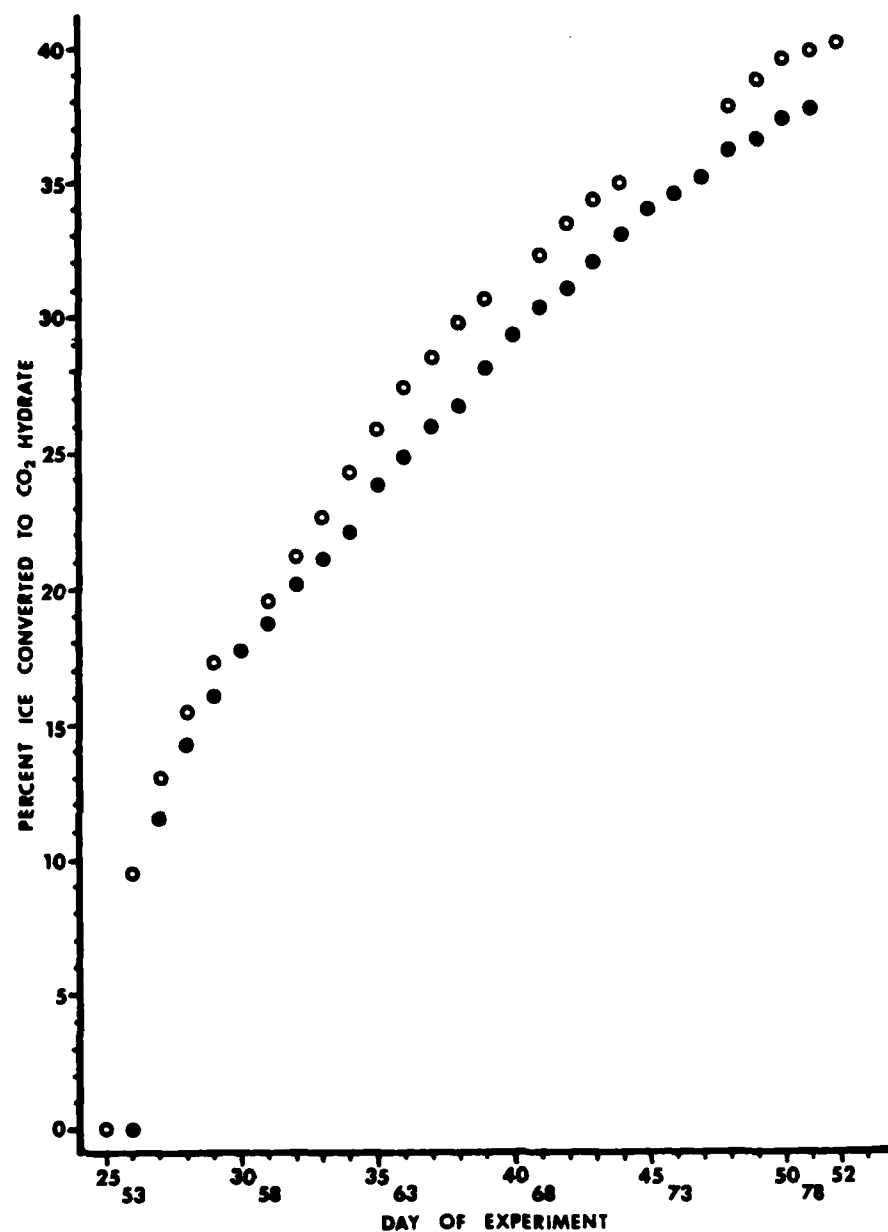


Figure 10. The percent ice converted to hydrate per day during the hydrate formation periods. The x-axis for the second formation period (Day 53-78) has been off-set to the right to allow separation of the data from that from the first formation period (Day 25-52). Circles are the data for Days 25-52. Dots are the data for Days 53-79.

concluded that the continuation of the hydrate formation periods longer than the time actually allowed would have resulted in about 5% additional ice converted to hydrate.

(2) The 40% conversion of the 8.93×10^{-1} moles of ice in the tube means 0.36 moles of ice converted to hydrate. Based on a reported density of ice at 213 K of 0.9252 g cm^{-3} (La Placa and Post, 1960), the 8.93×10^{-1} moles of ice occupied 17.4 cm^3 and the 0.36 moles of ice converted to hydrate occupied 6.95 cm^3 of that 17.4 cm^3 prior to conversion. Based on a 16% volume expansion when one mole of ice converts to hydrate, the 0.36 moles of ice expanded 5.72% or 0.4 cm^3 upon conversion to hydrate. Thus the volume occupied by the ice after 40% conversion to hydrate was 17.8 cm^3 . The volume of the aluminum tube (measured by filling the tube with water) was $40.0 \pm 0.5 \text{ cm}^3$. Therefore, even after the ice converted to hydrate, only 44.5% of the volume of the tube was filled. The remainder of the volume of the tube was pore (or void) space. This 55.5% void space was surprising as an effort had been made to place a maximum amount of ice in the tube.

(3) The large void space available in the tube allowed accommodation of the small volume expansion resulting from the 40% conversion of the ice to hydrate. Consequently, it was expected that the strain data would show no force exerted on the tube due to the conversion of the ice to hydrate.

(4) The reaction rate observed is much slower than that reported by Miller and Smythe (1970) for finely divided ice at comparable (but colder) temperatures. The slow reaction rate observed was attributed to poor ice- CO_2 atmosphere contact and to a change in the nature of the ice

from finely divided to more coarsely grained. The change in the nature of the ice was confirmed after the experiment. The ice was found to be a packed crystal mass with obvious pore spaces. The nature (size and packing) of the ice crystals is known to effect the formation rate (Miller, 1978; Miller and Smythe, 1970; Barrer and Edge, 1967). In general, the larger the ice crystals the slower the formation rate (Miller, 1978). Thus, the formation rate observed in the experiment may be the natural (unconfined) rate of formation for the nature of the ice used and not directly caused by the confinement of the ice in the tube. However, it probably was the confinement (or the loading of the ice) in the tube that changed the nature of the ice and therefore indirectly determined the formation rate.

Figures 11 and 12 present the strain data for the initial empty tube experiment and for the hydrate formation experiment. Figures 13 and 14 present the strain data for the control (argon + ice) experiment as well as the post-experiment empty tube data. The most favorable analysis of the data resulted in only 5×10^{-6} units of strain increase due to the hydrate formation. However, this is believed to be within the error of the experiment. The finding that no strain was caused by the hydrate formation is consistent with the amount of ice known to have been in the tube and with the void space available to accommodate the volume expansion resulting from the 40% conversion of the ice to hydrate.

Even though the experiment provided no answer to the question of whether or not the volume expansion accompanying the conversion of ice to hydrate is of geological importance on Mars, it did show that the conversion of ice to hydrate in confined spaces is a very slow reaction.

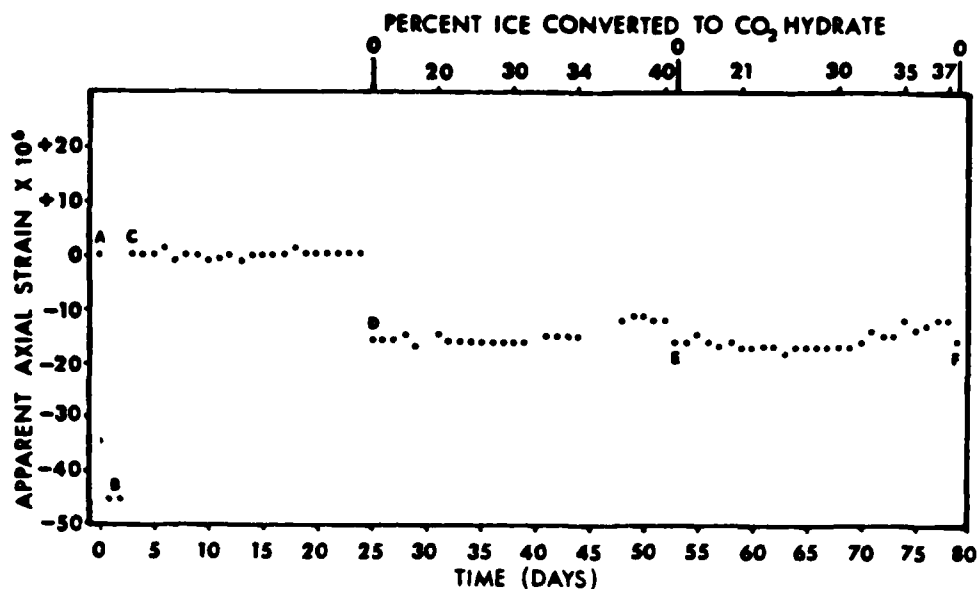


Figure 11. The axial strain data for the first empty tube experiment (Day 0-24) and for the hydrate formation experiment (Day 25-79). Point A is the axial strain at room temperature. Point B is the axial strain caused by temperature induced contraction of the tube (213 K and 5×10^{-3} mm Hg). The axial strain was instrumentally balanced to zero at 213 K and 5×10^{-3} mm Hg (Point C). Point D is the axial strain after the tube was loaded with ice (213 K and 5×10^{-3} mm Hg). Points E and F are the axial strain measurements after the hydrate was dissociated for the first and second hydrate formation periods, respectively.

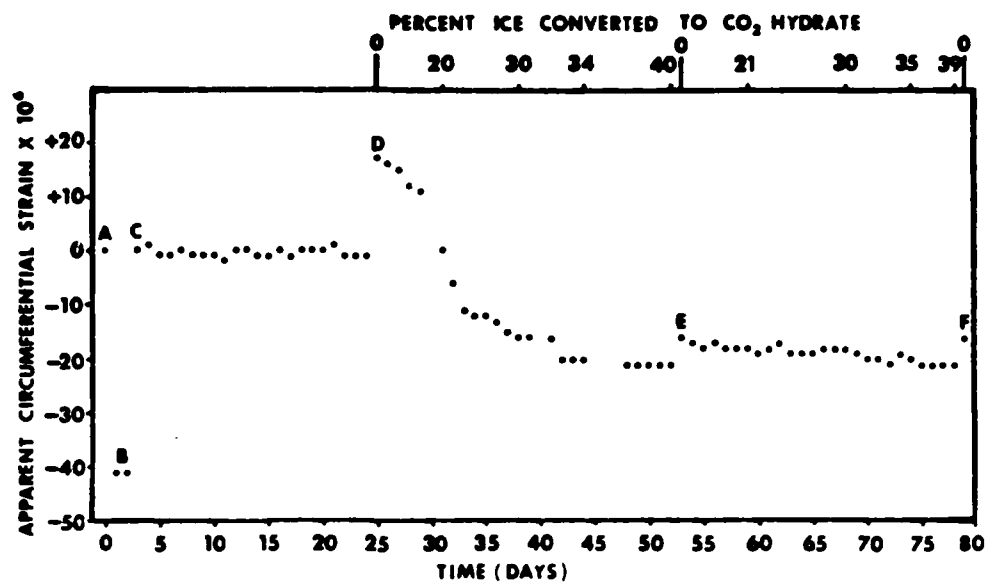


Figure 12. The circumferential strain data for the first empty tube experiment (Day 0-24) and for the hydrate formation experiment (Day 25-79). Point A is the circumferential strain at room temperature. Point B is the circumferential strain caused by temperature induced contraction of the tube (213 K and 5×10^{-3} mm Hg). Point C is the circumferential strain balanced to zero at 213 K and 5×10^{-3} mm Hg. Point D is the circumferential strain after the tube was filled with ice (213 K and 5×10^{-3} mm Hg). Points E and F are the circumferential strain measurements after the hydrate was dissociated for the first and second hydrate formation periods, respectively.

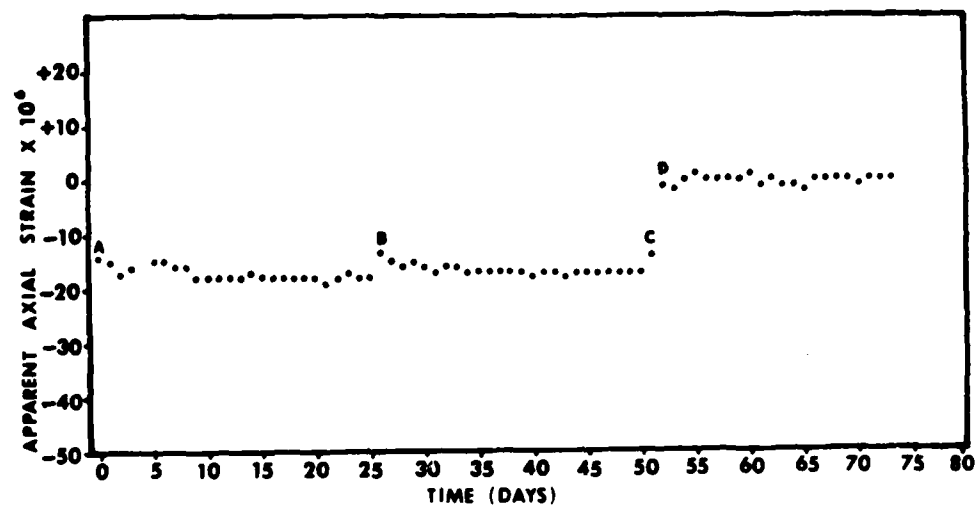


Figure 13. The axial strain data from the control experiment (Day 0-51) and from the second (post-experiment) empty tube experiment. Points A, B, and C are the strains measured at 213 K and 5×10^{-3} mm Hg. Point A is before the argon gas was added. Points B and C are after argon gas was removed. Point D marks the start of the empty tube experiment.

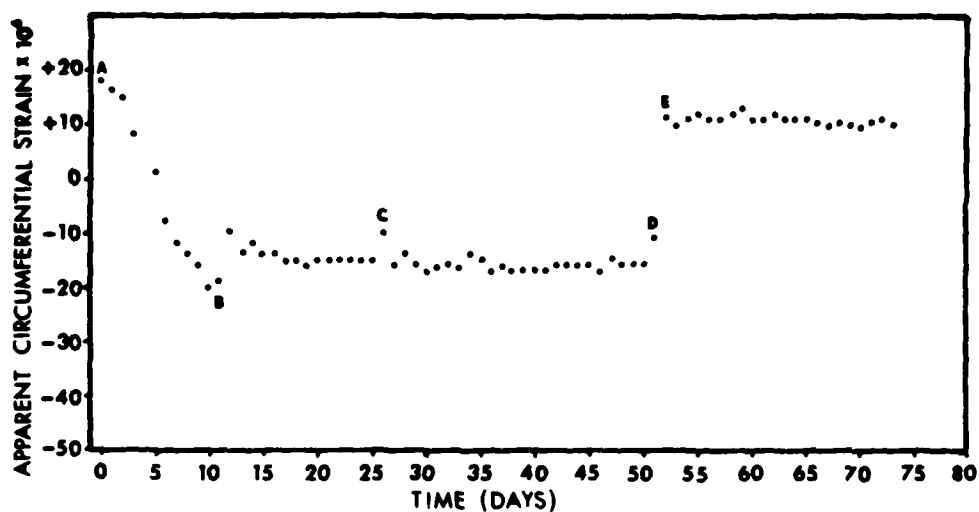


Figure 14. The circumferential strain data from the control experiment (Day 0-51) and from the second (post-experiment) empty tube experiment (Day 52-73). Points A, C, and D are the strains measured at 213 K and 5×10^{-3} mm Hg with the tube filled with ice. Point A is before argon gas was added. Points C and D are after the argon gas was removed. Point B indicates the most likely point where the circumferential gauge shifted $+11 \times 10^{-6}$ units of strain. Point E marks the start of the empty tube experiment and shows that a $+11 \times 10^{-6}$ shift in circumferential strain has occurred since the first empty tube experiment (Day 0-24, Figure 13).

There probably is a practical optimum that allows a maximum amount of ice to be packed in a confined space but still allows sufficient surface area for a 40% conversion to hydrate to occur in a reasonable period of time. A reasonable period of time would be a time shorter than the length of a Martian winter. If this practical optimum had been achieved in packing the tube used in the experiment, the rate of reaction may have been slower than that observed, but the volume expansion (on 40% conversion to hydrate) would have had a better opportunity to exert a force on the tube.

A calculation was made of the amount of ice required to give a volume, after 40% conversion to hydrate, greater than the known volume of the tube. It should be noted that the calculations assume:

(1) confinement does not affect the volume expansion of ice on conversion to hydrate;

(2) the volume expansion as ice converts to hydrate will cause the tube to expand as required.

Table 13 lists amounts of ice and the percent volume increase required of the tube to contain the ice after 40% conversion to hydrate.

A probable best case is as follows. If the tube was filled with a solid ice mass (40 cm^3 , which is equal to 2.05 moles at 213 K; see Table 13), the ice would form a cylinder with dimensions the same as the internal dimensions of the tube (internal diameter = 1.98 cm; length = 12.99 cm). If the surface of the ice cylinder converted to hydrate to a depth of 0.21 cm, an inner core of ice would remain. The dimensions of the ice core would be:

TABLE 13. Percent expansion of the tube required to accommodate a 40% conversion to hydrate of various amounts of ice at 213 K. Volume of the tube is 40 cm³. Volume change calculations are based on a 16% expansion in volume when one mole of ice converts to hydrate. The molar volume of ice at 213 K was taken as 19.47 cm³.

AMOUNT OF ICE IN TUBE (cm ³)	AMOUNT OF ICE IN TUBE (Moles)	AMOUNT OF ICE CONVERTED TO HYDRATE (Moles)	VOLUME OCCUPIED BY THE ICE AFTER CONVERSION TO HYDRATE	% EXPANSION REQUIRED OF TUBE TO ACCOMMODATE THE NEW VOLUME
38.0	1.95	0.78	39.90	0
38.5	1.98	0.79	40.45	1.13
39.0	2.00	0.80	41.00	2.50
39.5	2.03	0.81	41.54	3.85
40.0	2.05	0.82	42.10	5.25

$$\text{diameter} = 1.98 - 2(0.21) = 1.56 \text{ cm};$$

$$\text{length} = 12.99 - 2(0.21) = 12.57 \text{ cm}.$$

The volume of the ice core would be 24.03 cm^3 or 60% of the ice cylinder. Thus, 40% (or 0.82 moles) of the ice would be hydrate. From Table 13, the tube would be required to expand 5.25%.

The freezing of water is known to result in an expansion in the volume occupied by the water. This expansion is known to result in mechanical weathering, patterned ground, and ground heaving on Earth (Bloom, 1969). If the 40.0 cm^3 tube were filled with water and frozen at 213 K, the volume occupied by the resulting ice should be 43.22 cm^3 (the tube would be required to expand 8.08%). Figures 15 and 16 show the strains measured when the tube was filled with water and the water frozen at 213 K. The water was not totally confined as the top was left off the tube. However, the strains resulting were sufficient to rupture the tube. The calculated 5.25% expansion of the tube resulting from the 40% conversion of 40 cm^3 of ice to hydrate should result in comparable strains.

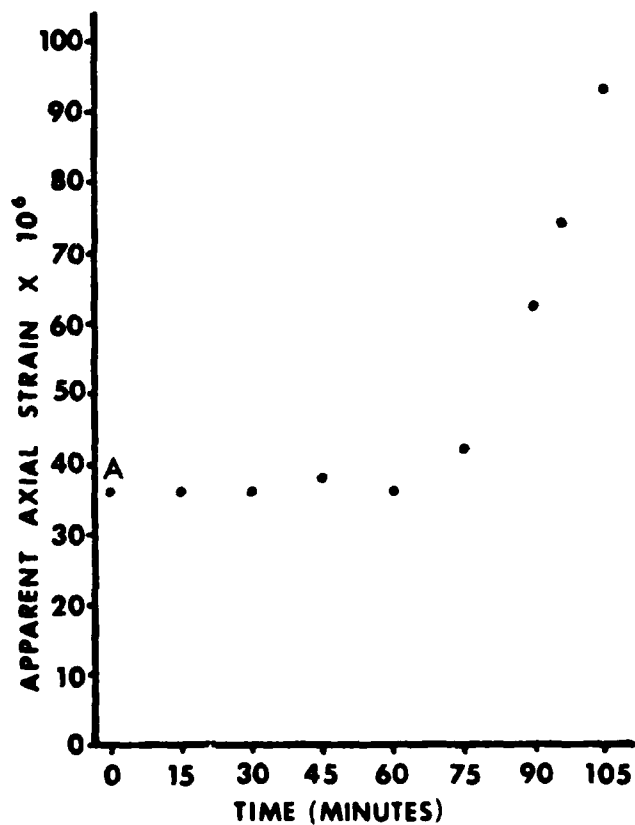


FIGURE 15. Axial strain performance during the freezing of 40 cm³ of water in the tube at 213 K. Point A represents the shift in strain (from zero at 213 K; empty tube) caused by filling the tube with water.

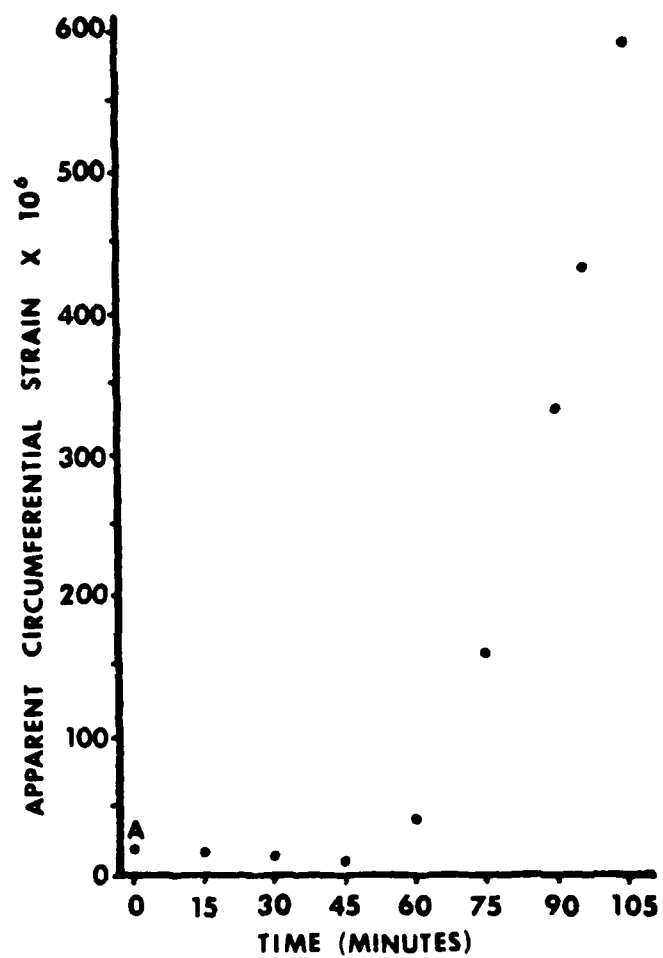


FIGURE 16. Circumferential strain performance during the freezing of 40 cm³ of water in the tube at 213 K. Point A represents the shift in strain (from zero at 213 K; empty tube) caused by filling the tube with water.

Summary

Apparent collapse features on Mars, such as the chaotic terrain, may be caused by the 14% volume decrease accompanying the conversion of a buried CO₂ hydrate deposit to ice. The chaotic terrain that appears to be the source areas for large flood channels may have been caused by the melting of buried ice or hydrate deposits. It may be possible to determine whether the melting of ice or hydrate formed a specific channel and chaotic terrain source area by:

- (1) calculating the dimensions of the buried deposit (as ice and as hydrate) from the amount of water required to form the channel;
- (2) comparing the calculated dimensions of the ice and hydrate deposit with the dimensions of the chaotic terrain source area.

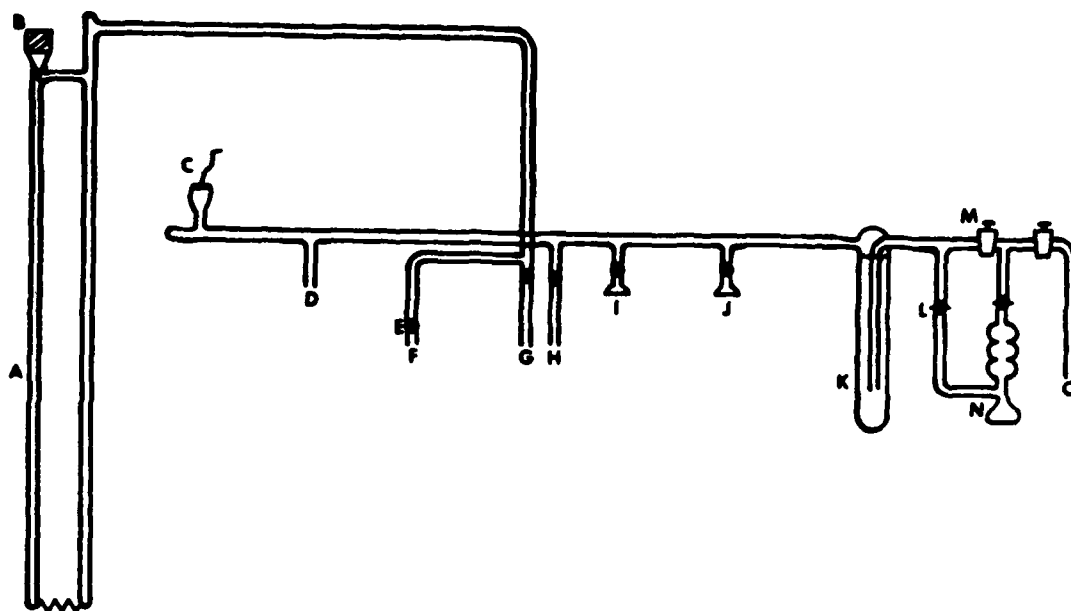
No experimental evidence was obtained to support the idea that the 16% volume expansion accompanying the conversion of ice to hydrate causes mechanical weathering, patterned ground, or ground heaving on Mars. Conversion of ice to hydrate was found to be possible in confined spaces provided sufficient time was allowed for the reaction. Calculations show that a solid ice cylinder (length 13 times radius), which fills a confined space, must convert to hydrate to a depth equal to 21% of its radius to cause a volume expansion approximately equal to that which occurs when water freezes to ice in the same space. Thus, theoretically, the volume expansion occurring when ice converts to hydrate could be a weathering and a geomorphological agent on Mars. Measurements of rates of reaction and of conversion limits for converting solid ice masses to

hydrate have not been made. Such measurements may show that the conversion process is not compatible with the duration of hydrate forming conditions on Mars. In addition, actual measurement of strains imparted to the walls confining a solid ice mass as it converts to hydrate is necessary to confirm the process as a possible weathering and geomorphological agent on Mars.

APPENDIX 1

Figure 17 shows the main glass vacuum line which was used for all experiments. The line was designed using as a guide the methods described by Shriver (1969). The vacuum was produced by a mercury diffusion pump and a rotary fore-pump. Pressure in the line was measured by a thermocouple gauge (for pressures lower than 1000 micrometers Hg) and by a mercury manometer. The use of teflon stopcocks and o-ring joints with clamps allowed the line to be used for low pressure and high pressure work. The mercury manometer allowed pressure measurement to 2.5 atmospheres.

Figure 18 shows the apparatus used to measure the rate of conversion of ice to CO_2 hydrate at 156 K. The chamber used was a glass double dewar. An o-ring joint (J) allowed the chamber to be sealed with a demountable brass electrical feedthrough (K). An electrical tape (D) was wrapped around the inner tube (C) of the double dewar chamber. The electrical leads (E and H) were fed through glass-kovar tubes (G) and the tubes soldered vacuum tight. The electrical leads were connected to a variable powerstat. The inner tube was sealed to an outer tube (B) by an o-ring joint and clamp (F). The space between the inner and outer tube was evacuated via line L and sealed by closing the teflon stopcock on the line. A glass manifold (Q) was made as part of the inner tube of the double dewar chamber. The double dewar and manifold were mounted so that line R (Figure 18) connected to line D (Figure 17) of the main vacuum line. Line P (Figure 18) connected to line F (Figure 17) of the mercury manometer.



- | | |
|------------------------|----------------------------|
| A - Mercury manometer | I - O-ring joint |
| B - Teflon stopcock | J - O-ring joint |
| C - Thermocouple gauge | K - Cold trap |
| D - Vacuum line | L - Glass stopcock |
| E - Teflon stopcock | M - Glass stopcock |
| F - Line to manometer | N - Mercury diffusion pump |
| G - Line to manometer | O - To rotary fore-pump |
| H - Vacuum line | |

FIGURE 17. Main glass vacuum manifold.

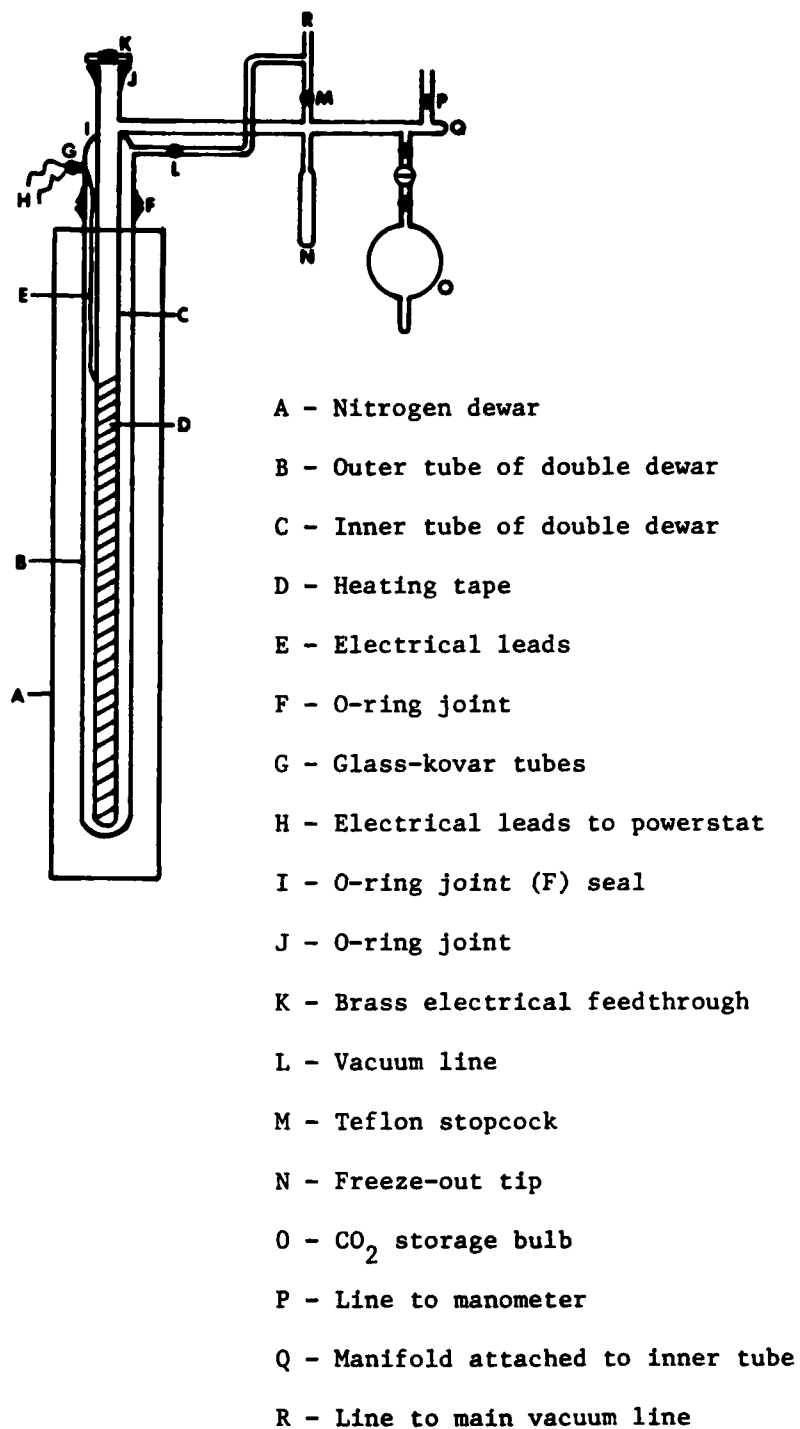


FIGURE 18. Apparatus used to measure the rate of conversion of ice to hydrate at 156 K.

The double dewar chamber was surrounded by a liquid nitrogen dewar (A). CO_2 gas was stored in bulb O. Transfer from the bulb to the chamber was facilitated by use of the freeze-out tip N. Temperature control for the experiment was accomplished by filling about two-thirds of the nitrogen dewar with liquid nitrogen and manually controlling the temperature by regulating the current flow through the heating tape (D) with the variable powerstat. The bulb used to transfer the water vapor to the chamber was attached to the main vacuum line (at o-ring joint I of Figure 17). The vapor was transferred through the main vacuum line and into the chamber. The chamber was then sealed-off from the main vacuum line by closing stopcock M. CO_2 was added from bulb O. Stopcock P, to the mercury manometer, was opened and the pressure decrease with time was recorded.

AD-A106 744

AIR FORCE INST OF TECH WRIGHT-PATTERSON AFB OH
THE OCCURRENCE AND GEOLOGICAL IMPLICATIONS OF CARBON DIOXIDE CL--ETC(U)
MAY 79 G A ARMISTEAD
AFIT-CI-79-257T

F/G 3/2

UNCLASSIFIED

NL

2+2
4106 744

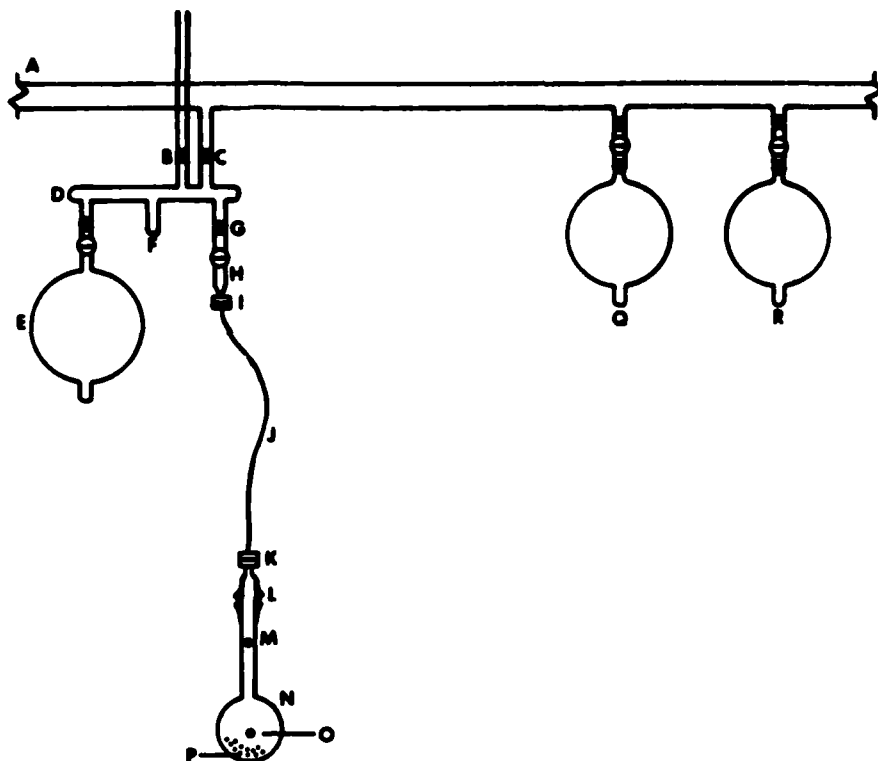


END
DATE
FILMED
11-81
DTIC

END
DATE
FILMED
11-81
DTIC

APPENDIX 2

The apparatus used to measure the volume expansion that occurs on conversion of ice to hydrate is shown in Figure 19. A section (A) of the main vacuum line is shown with 2 gas transfer bulbs attached (at o-ring joints I and J of Figure 17). A small glass manifold (D) was connected to the main vacuum line by line C (line H of Figure 17). Line B (line G of Figure 17) connected the apparatus to the mercury manometer. The reaction bulb was attached to the manifold with a flexible tube (J) by swage-lock union (I and K) to kovar-glass o-ring joints (H and L). The reaction bulb (N) was submersed in a nitrogen dewar (not shown) filled with an acetone-dry ice bath. Thermocouples attached to the reaction bulb at O and M provided temperature data. Known amounts of CO_2 were stored in bulbs E, Q, and R. Transfer of the stored CO_2 was facilitated by use of the freeze-out tip F.



A - Section of main vacuum line

B - Line to manometer

C - Line to main vacuum line

D - Manifold

E - Storage/transfer bulb

F - Freeze-out tip

G - Teflon stopcock

H - Kovar-glass o-ring joint

I - Swage-lock union

J - Flexible tubing

K - Swage-lock union

L - Kovar-glass o-ring joint

M - Thermocouple

N - Reaction bulb

O - Thermocouple

P - Steel ball bearings

Q - Storage/transfer bulb

R - Storage/transfer bulb

FIGURE 19. Apparatus used to measure the volume expansion that occurs on conversion of ice to hydrate.

APPENDIX 3

The apparatus used for the strain measurement experiment is identical to the apparatus shown in Figure 18 and described in Appendix 1. The temperature of the experiment (213 K) was established by filling the nitrogen dewar (A, Figure 18) with alcohol (2-propanol) and submerging the probe of a Neslab M-60 cryocooler in the alcohol. The heating tape (D, Figure 18) was not used. An o-ring clamp secured the electrical feedthrough (K, Figure 18) and allowed a pressure of up to 2.5 atmospheres in the chamber.

The procedure used to determine the percent ice converted to CO₂ hydrate during the experiment was as follows.

(1) After the tube containing the ice was placed in the chamber (at a temperature of 213 K) and a pressure of 5×10^{-3} mm Hg established, the known amount of CO₂ (3.23×10^{-1} moles) used for the experiment was allowed in the chamber by opening the stopcocks to storage bulb O (see Figure 18). The pressure was measured after 3 minutes at 1757.50 mm Hg for the first hydrate formation period and 1756.50 for the second hydrate formation period. The difference was considered negligible.

(2) The point, 1757.50 mm Hg caused by 3.23×10^{-1} moles of CO₂, and the point, zero pressure at zero moles, were used to construct line A of Figure 20. The line is represented by the equation:

$$\text{moles of CO}_2 = 1.84 \times 10^{-4} \times \text{Pressure.}$$

(3) The moles of CO₂ adsorbed during the experiment was determined by the equation:

$$\text{moles CO}_2 \text{ adsorbed} = 3.23 \times 10^{-1} - (1.84 \times 10^{-4} \times \text{Pressure}).$$

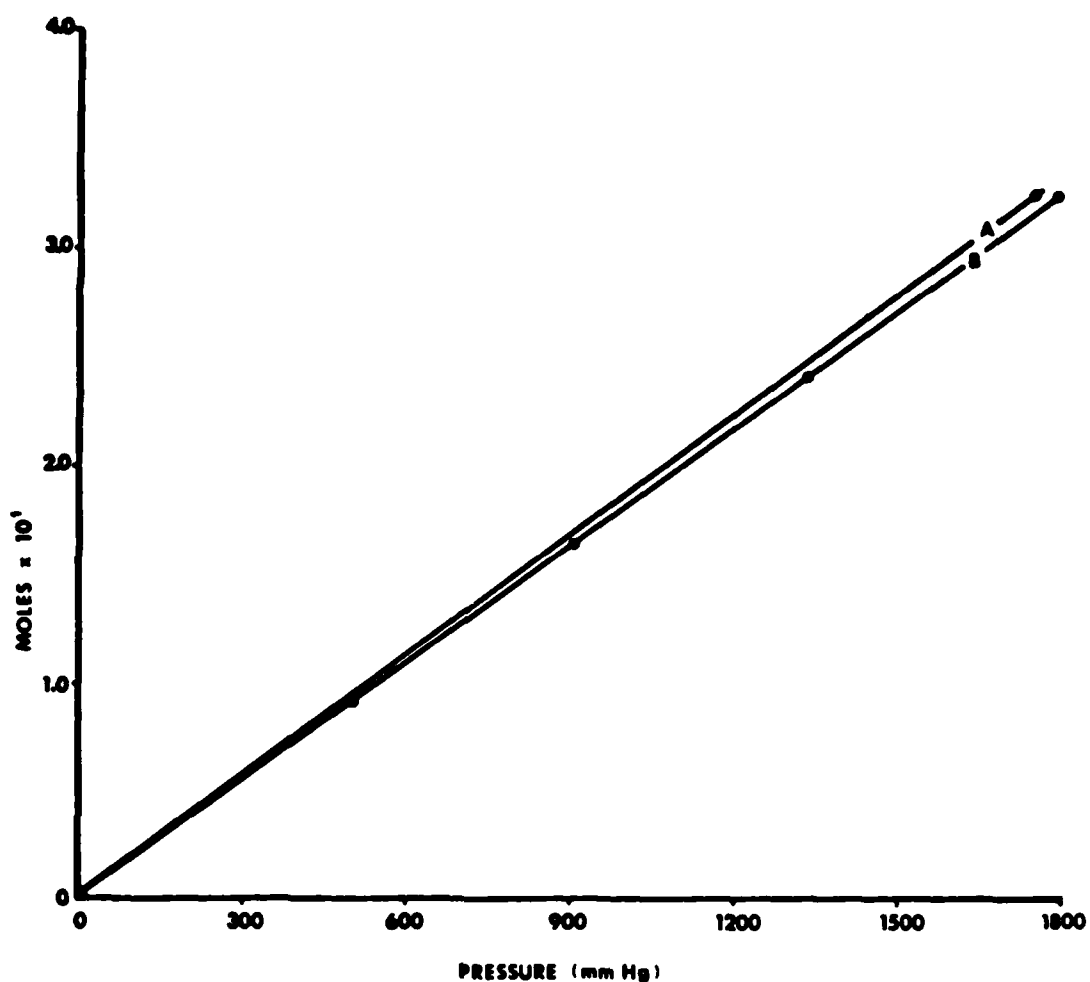


FIGURE 20. Line A represents the constructed line based on the data: 1757.50 mm Hg at 3.23×10^{-1} moles and zero pressure at zero moles. Line B represents the empty chamber-room temperature pressure-moles relationship.

(4) The percent ice converted to CO_2 hydrate (based on the formula $\text{CO}_2 \cdot 6\text{H}_2\text{O}$ and the known amount of ice used in the experiment, 8.93×10^{-1} moles) was determined from the equation:

$$\% \text{ ice converted} = \frac{\text{moles of } \text{CO}_2 \text{ adsorbed from (3)} \times 6 \times 100}{8.93 \times 10^{-1}} .$$

Confidence in Line A of Figure 20 was gained by determining the empty chamber-room temperature pressure-moles relationship (Line B, Figure 20). As can be seen, the chamber temperature and the volume decrease of the chamber (caused by the tube, ice, and wires) during the experiment shifted the pressure-moles relationship from line B to line A.

ACKNOWLEDGEMENT

The author wishes to acknowledge the advice and assistance of the thesis committee members: Dr. Elbert A. King, Dr. Stuart A. Hall, and Dr. Russell A. Geanangel. A special acknowledgement is due Dr. Carl Norman for his assistance in equipment preparation and data interpretation for the strain measurement experiments. Special thanks is given the following individuals for assistance in the design, fabrication, installation, and checkout of the experimental apparatus: Randy Wilkin, Ray Terhune, Vic Diatschenko, Dr. C.W. Chu, Dr. L. Wood, and Dr. R. Geanangel. A very special thanks is given my wife, Jeanie, for her preparation of all the Figures for the manuscript, and Diana Sandefur for typing the manuscript.

This research was made possible by the Air Force Institute of Technology, Civilian Institute Division, and by a grant of funds from the Geology Foundation, University of Houston.

REFERENCES

- Baker, V., Paleohydrology and sedimentology of Lake Missoula flooding in eastern Washington, Geol. Soc. America Spec. Paper 144, 79 pp.
- Barrer, R., and Edge, A., Gas hydrates containing argon, krypton and xenon: kinetics and energetics of formation and equilibria, Proc. Roy. Soc. Ser. A, 300, 1, 1967.
- Barrer, R., and Ruzicka, D., Non-stoichiometric Clathrate compounds of water: Part 4 -- Kinetics of formation of clathrate phases, Trans. Faraday Soc., 58, 2262, 1962.
- Barrer, R.M., and Stuart, W.I., Nonstoichiometric clathrate compounds of water, Proc. Roy. Soc. Ser. A., 243, 172, 1957.
- Bloom, A., The Surface of the Earth, 152 pp., Prentice-Hall, Inc., Englewood Cliffs, New Jersey, 1969.
- Bouzat, A., and Azinieres, L., Composition de l'hydrate de chlore, Bull. Soc. Chim. France, 35, 545, 1924.
- Briggs, G., The nature of the residual Martian polar caps, Icarus, 23, 167, 1974.
- Carr, M., and Schaber, G., Martian permafrost features, J. Geophys. Res., 82, 4039, 1977.
- Chase, S., Hatzenbeler, H., Kieffer, H., Miner, E., Munch, G., and Neugebauer, G., Infrared radiometry on Mariner 9, Science, 175, 308, 1972.
- Claussen, W.F., Suggested structures of water in inert gas hydrates, J. Chem. Phys., 19, 159, 1951a.
- Claussen, W.F., Erratum: suggested structures of water in inert gas hydrates, J. Chem. Phys., 19, 662, 1951b.
- Claussen, W.F., A second water structure for inert gas hydrates, Jour. Chem. Phys., 19, 1425, 1951c.
- Cole, R., Dissertation, University of Illinois, Urbana, 1952.
- Cross, C., The heat balance of the Martian polar caps, Icarus, 15, 110, 1971.
- Davidson, D.W., Clathrate Hydrates, in Water: A Comprehensive Treatise, edited by F. Franks, vol. 2, pp. 115-234, Plenum Press, New York, 1973.

- Davy, H., On some of the combinations of oxy-muriatic gas and oxygen and on the chemical relations of the principals to inflammable bodies, Phil. Trans. Roy. Soc., London, 101, 1, 1811.
- Deaton, W.M., and Frost, E.M., Gas hydrates and their relation to the operation of natural-gas pipe lines, U.S. Bureau of Mines Mono., No. 8, 1946.
- Delsemme, A.H., and Miller, D.C., Physico-chemical phenomena in comets--II. Gas adsorption in snows of the nucleus, Planet. Space Sci., 18, 717, 1970.
- Delsemme, A.H., Swings, P., Hydrates de gas dans les noyaux cometaires et les grains interstellaires, Ann. Astrophys., 15, 1, 1952.
- Delsemme, A.H., and Wegner, A., Physico-chemical phenomena in comets--I. Experimental study of snows in a cometary environment, Planet. Space Sci., 18, 709, 1970.
- Dobrovolskis, A., and Ingersoll, A., Carbon dioxide - water clathrate as a reservoir of CO₂ on Mars, Icarus, 26, 353, 1975.
- Eisenberg, D., and Kauzmann, W., The Structure and Properties of Water, 296 pp., Oxford University Press, New York and Oxford, 1969.
- Fanale, F., and Cannon, W., Mars: The role of the regolith in determining atmospheric pressure and the atmosphere's response to insolation changes, J. Geophys. Res., 83, 2321, 1978.
- Fanale, F., and Cannon, W., Exchange of adsorbed H₂O and CO₂ between the regolith and atmosphere of Mars caused by changes in surface insolation, J. Geophys. Res., 79, 3397, 1974.
- Fanale, F., and Cannon, W., Adsorption on the Martian regolith, Nature, 230, 502, 1971.
- Forcrand, R. De, Sur la composition des hydrates de gaz, Acad. Sci. Paris, Comptes rendus, 134, 835, 1902.
- Frost, E.M., and Deaton, W.M., Gas hydrate composition and equilibrium data, Oil and Gas Jour., 45, 170, 1946.
- Gierasch, P., and Toon, O., Atmospheric pressure variations and the atmosphere of Mars, J. Atmos. Sci. 30, 1502, 1973.
- Hammerschmidt, E.G., Formation of gas hydrates in natural gas transmission lines, Ind. Eng. Chem., 26, 851, 1034.

- Hempel, W., and Seidel, J., *Über Verbindungen des Kohlendioxyds mit Wasser, Athylather und Alkoholen*, *Berichte*, 31, 2997, 1898.
- Henry, R.M., *Personal communication*, 1979.
- Herr, K.C., and Pementel, G.C., *Infrared adsorptions near three microns recorded over the polar cap of Mars*, *Science*, 166, 496, 1969.
- Herreilers, H.W., *Dissertation*, University of Amsterdam, 1936.
- Hess, S., Henry, R., Leovy, C., Ryan, J., and Tillman, J., *Meteorological results from the surface of Mars: Viking 1 and 2*, *J. Geophys. Res.* 82, 4559, 1977.
- Ingersoll, A., *Mars: The case against permanent CO₂ frost caps*, *J. Geophys. Res.*, 79, 3403, 1974.
- Ingersoll, A., and Leovy, C., *The atmospheres of Mars and Venus*, *Annu. Rev. Astron. Astrophys.*, 9, 147, 1971.
- Jeffrey, G.A., and McMullan, R.K., *The clathrate hydrates*, *Prog. Inorg. Chem.*, 8, 43, 1967.
- Jones, K., Arvidson, R., Guinness, E., Bragg, S., Wall, S., Carlston, C., and Pidek, D., *One Mars year: Viking lander imaging observations of sediment transport and H₂O-condensates*, submitted to *Science*, Sept. 8, 1978.
- Khoroshilov, V.A., Deggyarev, B.V., and Bukhgalter, E.B., *Gazov. Prom.*, 15(11), 18, 1970.
- Kieffer, H., *Soil surface temperatures at the Viking lander sites*, *Science*, 194, 1344, 1976.
- Kieffer, H., Chase, S., Martin, T., Miner, E., and Palluconi, F., *Martian north pole summer temperatures: Dirty water ice*, *Science*, 194, 1341, 1976.
- Kieffer, H., Martin, T., Peterfreund, A., and Jakosky, B., *Thermal and albedo mapping of Mars during the Viking primary mission*, *J. Geophys. Res.* 82, 4249, 1977.
- Kieffer, H., and Palluconi, F., *The climate of the Martian Polar Cap*, paper presented at the *Second International Colloquium on Mars*, Calif. Inst. of Tech., Jet Propul. Lab., Pasadena, Calif., Jan. 15-18, 1979.

- Kliore, A., Cain, D., Fjeldbo, G., Seidel, B., and Sykes, M., The atmosphere of Mars from Mariner 9 radio occultation measurements, *Icarus*, 17, 484, 1972.
- Kliore, A., Fjeldbo, G., and Seidel, B., Mariners 6 and 7: Radio occultation measurements of the atmosphere of Mars, *Science*, 166, 1393, 1969.
- La Placa, S., and Post, B., Thermal expansion of ice, *Acta Crystallogr.*, 13, 503, 1960.
- Larson, S.D., 1955, Phase studies of the two component carbon dioxide-water system involving the carbon dioxide hydrate: Ann Arbor, Mich., Doctoral Dissertation Publ. No. 15235, Univ. Microfilms, 84 pp.
- Leovy, C., Mars ice caps, *Science*, 154, 1178, 1966.
- Lewis, J.S., The clouds of Jupiter and $\text{NH}_3\text{-H}_2\text{O}$ and $\text{NH}_3\text{-H}_2\text{S}$ system, *Icarus*, 10, 365, 1969.
- Mak, T.C., and McMullan, R.K., Polyhedral clathrate hydrates X. Structure of the double hydrate of tetrahydrofuran and hydrogen sulfide, *J. Chem. Phys.*, 42, 2732, 1965.
- Makogon, Yu. F., Trebin, F.A., Trofimuk, A.A., Tsarev, V.P., and Cherskiy, N.V., Detection of a pool of natural gas in a solid (hydrate gas) state, *Dokl. Akad. Nauk SSSR (Earth Sci.)*, English Transl., 196, 203, 1971.
- Maxwell, T., Otto, E., Picard, M., and Wilson, R., Meteorite impact: a suggestion for the origin of some stream channels on Mars, *Geology*, 1, 9, 1973.
- McCauley, J., Carr, M., Cutts, J., Hartmann, W., Masursky, H., Milton, D., Sharp, R., and Wilhelms, D., Preliminary Mariner 9 report on the geology of Mars, *Icarus*, 17, 289, 1972.
- McKoy, V., and Sinanoglu, O., Theory of dissociation pressures of some gas hydrates, *J. Chem. Phys.*, 38, 2946, 1963.
- Miller, J.P., A portion of the system calcium carbonate-carbon dioxide-water with geological implications, *Am. Jour. Sci.*, 250, 161, 1952.
- Miller, S.L., Personal communication, 1978.

- Miller, S.L., The nature and occurrence of clathrate hydrates, in Natural Gases in Marine Sediments, edited by I.R. Kaplan, pp. 151-177, Plenum Press, New York, 1974.
- Miller, S.L., Clathrate hydrates of air in Antarctic ice, *Science*, 165, 489, 1969.
- Miller, S.L., The occurrence of gas hydrates in the solar system, *Proc. Nat. Acad. Sci. U.S.*, 47, 1798, 1961.
- Miller, S.L., and Smythe, W.D., Carbon Dioxide clathrate in the Martian ice cap, *Science*, 170, 531, 1970.
- Milton, D., Carbon dioxide hydrate and floods on Mars, *Science*, 183, 654, 1974.
- Milton, D., Water and processes of degradation in the Martian landscape, *J. Geophys. Res.*, 78, 4037, 1973.
- Murray, B., and Malin, M., Polar volatiles on Mars -- Theory versus observation, *Science*, 182, 437, 1973.
- Murray, B., Soderblom, L., Cutts, J., Sharp, R., Milton, D., and Leighton, R., Geological framework of the south polar region of Mars, *Icarus*, 17, 328, 1972.
- Mutch, T.A., Arvidson, R.E., Head, J.W., Jones, K.L., and Saunders, R.S., The Geology of Mars, 400 pp., Princeton University Press, Princeton, New Jersey, 1976.
- Neugebauer, G., Munch, G., Chase, S.C., Hatzenbeler, H., Miner, E., and Schofield, D., Mariner 1969: Preliminary results of the infrared radiometer experiment, *Science*, 196, 98, 1969.
- Neugebauer, G., Munch, G., Kieffer, H., Chase, C., Miner, E., and Schofield, D., Mariner 1969 infrared radiometer results: Temperatures and thermal properties of the Martian surface, *Astron. J.*, 76, 719, 1971.
- Pauling, L. and Marsh, R.E., The structure of chlorine hydrate, *Proc. Nat. Acad. Sci. U.S.*, 38, 112, 1952.
- Peale, S., Schubert, G., and Lingenfelter, R., Origin of Martian channels: Clathrates and water, *Science*, 184, 273, 1975.
- Ryan, J., Personal communication, 1979.

- Ryan, J.A., and Henry, R.M., Personal communication. All pressure, temperature, and uncertainty data from personal communication, Viking Meteorology Science Team, 1979.
- Sagan, C., Liquid carbon dioxide and the Martian polar laminas, J. Geophys. Res., 78, 4250, 1973.
- Sagan, C., Toon, O., Gierasch, P., Climatic change on Mars, Science, 181, 1045, 1973.
- Schroeder, W., Sammlung Chem. Chem.-Tech. Vortrage 29, 1, 1926.
- Sharp, R., Ice on Mars, Jour. Glaciology, 13, 173, 1974.
- Sharp, R., Mars: fretted and chaotic terrains, J. Geophys. Res., 78, 4073, 1973.
- Sharp, R., Soderblom, L., Murray, B., and Cutts, J., The surface of Mars. 2--uncratered terrains, J. Geophys. Res., 76, 331, 1971.
- Sill, G.T., and Wilkening, L.L., Ice clathrate as a possible source of the atmospheres of the terrestrial planets, Icarus, 33, 13, 1978.
- Smythe, W.D., Spectra of hydrate frosts: Their application to the outer solar system, Icarus, 24, 421.
- Soderblom, L., Malin, M., Cutts, J., and Murray, B., Mariner 9 observations of the surface of Mars in the north polar region, J. Geophys. Res., 78, 4197, 1973.
- Shriver, D., The Manipulation of Air-Sensitive Compounds, 299 pp., McGraw-Hill Book Company, New York, 1969.
- Stackelberg, M. von, Feste gashydrate, Naturwissen-schaften, 36, 327, 1949a.
- Stackelberg, M. von, Feste gashydrate, Naturwissen-schaften, 36, 359, 1949b.
- Stackelberg, M. von, and Frubuss, H., Feste gashydrate. IV. Doppelhydrate, Z. Elektrochem., 58, 99, 1954.
- Stackelberg, M. von, and Jahns, W., Feste gashydrate. IV. Die Gitterauf-weitungsarbeit, Z. Elektrochem., 58, 162, 1954.
- Stackelberg, M. von, and Meinhold, W., Feste gashydrate III. Mischhydrate, Z. Elektrochem., 58, 40, 1954.

- Stackelberg, M. von, and Muller, H.R., Feste gashydrate II. Struktur und Rauchemie, Z. Elektrochem., 58, 25, 1954.
- Stackelberg, M. von, Muller, H.R., On the structure of gas hydrates, J. Chem. Phys., 19, 1319, 1951.
- Stoll, R.D., Ewing, J., and Bryan, G.M., Anomalous wave velocities in sediments containing gas hydrates, J. Geophys. Res., 76, 2090, 1971.
- Takenouchi, S., and Kennedy, G.C., Dissociation pressures of the phase CO_2 5-3/4 H_2O , J. Geol., 73, 383, 1965.
- Takenouchi, S., Kennedy, G., The binary system $\text{H}_2\text{O}-\text{CO}_2$ at high temperatures and pressures, American Jour. Sci., 262, 1055, 1964.
- Tamman, G., and Krige, G.J., Die Gleichgewichtsdrucke von gashydraten, Zeit. anorg. und allgem. Chem., 146, 179, 1925.
- Unruh, C.H., and Katz, D.L., Gas hydrates of carbon dioxide-methane mixtures, Jour. Petrol. Tech., 1, 83, 1949.
- Urey, H.C., Handbuch der Physik, edited by S. Flugge, v. 52, p. 363, Springer-Verlag, Berlin, 1959.
- van der Waals, J.H., and Platteeuw, J.C., Clathrate solutions, Advan. Chem. Phys., 2, 1, 1959.
- Villard, M.P., Etude experimentale des hydrates de gaz, Ann. Chim. Phys. (7), 11, 353, 1897.
- Villard, M.P. Sur l'hydrate carbonique et la composition des hydrates de gaz, Acad. Sci. Paris, Comptes rendus, 119, 368, 1894.
- Ward, W., Climatic variations on Mars. 1. Astronomical theory of insolation, J. Geophys. Res., 79, 3375, 1974.
- Ward, W., Murray, B., and Malin, M., Climatic variations on Mars: Evolution of carbon dioxide atmosphere and polar caps, J. Geophys. Res., 79, 3387, 1974.
- Wiebe, R., and Gaddy, V.L., The solubility of carbon dioxide in water at various temperatures from 12° to 40° and at pressures to 500 atm., Jour. Am. Chem. Soc., 62, 815, 1940.

Woiceshyn, P., Global seasonal atmospheric fluctuations on Mars,
Icarus, 22, 325, 1974.

Wroblewski, S., Sur la combinaison de l'acide carbonique et de
l'eau, Acad. Sci. Paris, Comptes rendus, 94, 212, 1882a.

Wroblewski, S., Sur la composition de l'acide carbonique hydrate,
Acad. Sci. Paris, Comptes rendus, 94, 954, 1882b.



